

N O T I C E

THIS DOCUMENT HAS BEEN REPRODUCED FROM
MICROFICHE. ALTHOUGH IT IS RECOGNIZED THAT
CERTAIN PORTIONS ARE ILLEGIBLE, IT IS BEING RELEASED
IN THE INTEREST OF MAKING AVAILABLE AS MUCH
INFORMATION AS POSSIBLE

NASA TECHNICAL MEMORANDUM

NASA TM-78311

(NASA-TM-78311) ELECTRICAL TORQUES ON THE
ELECTROSTATIC GYRO IN THE GYRO RELATIVITY
EXPERIMENT (NASA) 66 p HC A04/MF A01

N81-10344

CSSL 14B

G3/35

Unclass
29068

ELECTRICAL TORQUES ON THE ELECTROSTATIC GYRO IN THE GYRO RELATIVITY EXPERIMENT

By Peter Eby and Wesley Darbro
Space Sciences Laboratory

October 1980

NASA



*George C. Marshall Space Flight Center
Marshall Space Flight Center, Alabama*

TABLE OF CONTENTS

	Page
I. INTRODUCTION	1
II. GENERAL DISCUSSION OF ELECTROSTATIC TORQUES	3
III. EXPANSION OF THE ROTOR SHAPE IN HARMONICS	7
IV. TORQUES IN TERMS OF HARMONICS	14
V. EXACT NUMERICAL CALCULATION OF TORQUES	25
VI. NUMERICAL RESULTS	28
VII. TORQUE ON A GIMBALED GYRO INCLUDING ALL THE HARMONICS	31
VIII. SECONDARY TORQUES	36
IX. ORBITAL AVERAGING OF GRAVITY GRADIENT FORCES	39
X. AVERAGING OF TORQUES DUE TO SPACECRAFT ROLL	44
XI. SPIN AVERAGING	47
XII. CONCLUSION	48
REFERENCES	49
APPENDIX	51

PRECEDING PAGE BLANK NOT FILMED

LIST OF ILLUSTRATIONS

Figure	Title	Page
1.	Deviation from sphericity, Case I	8
2.	Deviation from sphericity, Case II	9
3.	Deviation from sphericity, Case III	10
4.	Size of harmonics, Case I	11
5.	Size of harmonics, Case II	12
6.	Size of harmonics, Case III	13
7.	Second harmonic torque versus angle	16
8.	Third harmonic torque versus angle	17
9.	Fourth harmonic torque versus angle	18
10.	Fifth harmonic torque versus angle	19

LIST OF SYMBOLS

\bar{T}	Torque vector
$\vec{i}, \vec{j}, \vec{k}$	Orthogonal unit vectors in rotor axes
$\hat{F}_x, \hat{F}_y, \hat{F}_z$	Orthogonal unit vectors in electrode axes
V_i	Voltage on ith electrode ($i = x, y, \text{ or } z$)
θ_o, ϕ_o	Polar and azimuthal angles of rotor spin vector in electrode axes
θ'	Angle between rotor spin vector and integration point on electrodes
d_o	Nominal rotor electrode gap
Δd	Variation in rotor electrode gap
α, β, γ	Direction cosines of integration point on electrodes
$\alpha_o, \beta_o, \gamma_o$	Direction cosines of rotor spin vector
r_o	Nominal rotor radius
ϵ_o	Permittivity constant
$r(\theta')$	Rotor shape as function of θ'
θ_1	Electrode half angle
M_i	$\frac{\epsilon_o r_o^2}{2 d_o^2} (V_{i+}^2 - V_{i-}^2)$ (+ and - refer to opposite electrodes)
P_i	$\frac{\epsilon_o r_o^2}{2 d_o^2} (V_{i+}^2 + V_{i-}^2)$
h_i	Preload along ith axis
f_i	Acceleration along ith axis
z	Difference in preloads for different axes
t	Miscentering
θ	Misalignment angle

TECHNICAL MEMORANDUM

ELECTRICAL TORQUES ON THE ELECTROSTATIC GYRO IN THE GYRO RELATIVITY EXPERIMENT

I. INTRODUCTION

The ultimate accuracy of an electrostatic gyro is determined by the level to which the Newtonian electrical torques can be reduced. An understanding of these torques is necessary for extrapolation of performance in a one-g environment to that expected in a nearly zero-g environment. The success of the Stanford Gyro Experiment depends on the reduction of all Newtonian gyro drifts to levels well below the relativity drifts, which are expected to be 7 arc sec/yr and 0.05 arc sec/yr for the geodetic and motional effects, respectively. It is important, first, to determine whether this is feasible and, second, to predict the accuracy to which the relativity effects can be measured, since this is important in assessing the relative desirability of performing the gyro experiment vis a vis other experimental tests of relativity theory. In addition, it is important to know the level of gyro performance on the ground at which a successful space experiment can be undertaken. For all these reasons, we give a general derivation of expressions for the torque on an electrostatic gyro from first principles. We also give a complete discussion of the subject, including numerical estimates of the torques for current state-of-the-art rotors. The various averaging effects are also discussed.

This report relies heavily on work done by Honeywell [1]. In Section II, we sketch the derivation of the basic torque equation derived in Reference 1. In Section III, we describe the sample rotors used for the purpose of our calculation. Section IV gives expressions for the torque in terms of the lower harmonics. These expressions are similar to those of Reference 1 but are those appropriate for circular electrodes. Section V gives the basic method of exact numerical integration we have developed and represents the main extension of the method of Reference 1. Our method includes the effect of all the higher harmonics up to the 20th. These harmonics are shown to be important and should be included in the calculation because some of the symmetry properties of the lower harmonics may not persist in the higher ones. Also, the Fourier series used in Reference 1 does not converge very rapidly. Numerical results for the three sample rotors are given in Section VI. Section VII gives results for the special case of a gimbaled gyro. This is not the actual configuration planned for the gyro experiments, but it illustrates the large reduction in torques for the gimbaled case. Section VIII describes how the method of Section V can be extended to secondary torques, i.e., those due to nonuniformity of the rotor electrode gap. The secondary torques are not calculated numerically in this report, but their magnitude

is estimated. The remaining sections describe the three averaging effects: the orbital averaging (Section IX), the averaging due to spacecraft roll (Section X), and the averaging due to rotor spin (Section XI). The orbital averaging combined with spacecraft roll is shown to be effective for two of the three components of gravity gradient force, and the third component can be minimized by proper design of the spacecraft. The averaging due to spacecraft roll is shown to be effective for the primary torques and is crucial for the achievement of the goal of 1 milliarcsec/yr drift for the gyro. The averaging due to spin is described but not calculated, since a complete map of the rotor is not yet available. Section XII states the conclusions of the report.

II. GENERAL DISCUSSION OF ELECTROSTATIC TORQUES

For a conductor in an external electric field \vec{E} , the force per unit area f is given by [1]

$$f = \frac{\epsilon_0}{2} |\vec{E}|^2$$

where $\epsilon_0 = 8.85 \times 10^{-12}$ farads/m. The electric field is perpendicular to the surface of the conductor and zero inside the conductor. If we consider an irregularly shaped conductor, then the total force \vec{F} and torque \vec{T} are given by

$$\vec{F} = \frac{\epsilon_0}{2} \oint_S |\vec{E}|^2 \vec{n} \, dS \quad (1)$$

$$\vec{T} = \frac{\epsilon_0}{2} \oint_S |\vec{E}|^2 (\vec{r} \times \vec{n}) \, dS \quad (2)$$

where the integral is taken over the entire surface S , \vec{n} is a unit vector normal to the surface, and \vec{r} is a vector from some origin to the surface element dS . It is important to realize that \vec{T} is dependent on our choice of origin. The evaluation of electric torques on a gyro is accomplished by choosing a suitable model for the actual shape of the gyro and calculating the integral in equation (2). For a perfectly spherical gyro $\vec{T} = 0$, as is obvious from equation (2).

To calculate \vec{T} we need to make several assumptions, the validity of which we now discuss.

a) The rotor shape is symmetrical about its spin axis. This certainly appears reasonable if the rotor is spinning sufficiently fast, since the irregularities would then average out over many rotations of the rotor. Honeywell [1] has produced an argument which shows that this is, in fact, true if one has a sufficiently smooth rotor (see Section XI). There is one important exception, however, and that is for a rotor with radial mass unbalance perpendicular to the spin axis. In

this case, the suspension forces can have an oscillatory component at the spin rate frequency and the radial mass unbalance torque does not average to zero. There is then present a torque component parallel to the spin axis which alters spin speed and can cause run-down.

b) The rotor shape can be represented by a cosine series of the form

$$r(\theta) = r_0 + \sum_{n=2}^{\infty} a_n \cos(n\theta) \quad (3)$$

Almost any shape can be so represented, and the number of terms needed is related to the dimensions of the radial irregularities as discussed in Section III. A derivation that does not assume this is given in Section V.

c) The electric field at a given point in the rotor electrode gap is given by $|\vec{E}| = V/d$, where d is the rotor electrode distance at that point and V is the rotor electrode potential. The justification for this is that the rotor electrode gap is so small (1500 $\mu\text{in.}$ typical) that one can treat the situation locally as a parallel plate in which the electric field is uniform. Honeywell [1] has made some calculations that bear this out.

d) Electrode edge effects can be neglected. It is difficult to estimate how good this assumption is, but it is probably much better for hexahedral electrodes than circular electrodes.

e) The variations in rotor electrode gap Δd defined by $d = d_0 + \Delta d$ satisfy the conditions

$$\frac{\Delta d}{d_0} \ll 1 \quad (4)$$

This is a good assumption, since the main contributor to Δd is the centering errors which are of order 15 $\mu\text{in.}$, giving

$$\frac{\Delta d}{d_0} \approx 0.01$$

Given all these assumptions, one can write the expression for \vec{T} in the form

$$\vec{T} = \frac{\epsilon_0 r_0^2}{2 d_0^2} \sum_i V_i^2 \iint_{S_i} \left(1 - \frac{2\Delta d}{d_0}\right) \frac{dr(\theta')}{d\theta'} (\vec{i}' \sin \phi' - \vec{j}' \cos \phi') \sin \theta' d\theta' d\phi' \quad (5)$$

where the sum is taken over the six electrodes and θ' , ϕ' are spherical coordinates defined about the gyro spin axis. This follows directly from equation (2). We have used equation (4) and expanded the $1/d^2$ term, set $r = r_0$ in the term $dS = r^2 \sin \theta' d\theta' d\phi'$, and expressed the surface integral as a sum of integrals over electrodes at potentials V_i . The expression for $(\vec{r} \times \vec{n})$ is justified by noting that it must be tangent to a latitude line; i.e., in the direction given by the unit vector $\vec{i}' \sin \phi' - \vec{j}' \cos \phi'$ and of magnitude equal to the (small) angle between the radius vector and the normal vector to a curve $dr/d\theta'$ (this is worked out in elementary calculus).

The integral in equation (5) is in a spherical coordinate system defined by the rotor spin axis tipped at an arbitrary angle with respect to the electrode axes. Since we must calculate the surface integrals in a coordinate system defined by the electrode axes, we need to transform equation (5) to this coordinate system. If (θ_0, ϕ_0) represents the orientation of the spin axis in these coordinates, then

$$\vec{i}' = \cos \theta_0 \cos \phi_0 \hat{F}_x + \cos \theta_0 \sin \phi_0 \hat{F}_y - \sin \theta_0 \hat{F}_z$$

$$\vec{j}' = -\sin \phi_0 \hat{F}_x + \cos \phi_0 \hat{F}_y$$

$$\cos \phi' = \frac{1}{\sin \theta'} [\sin \theta \cos \theta_0 \cos (\phi - \phi_0) - \cos \theta \sin \theta_0]$$

$$\sin \phi' = \frac{1}{\sin \theta'} [\sin \theta \sin (\phi - \phi_0)]$$

define the relationship between the primed and unprimed angles. The first two equations follow from the fact that the vector in the spin axis direction is

$$\hat{\mathbf{k}} = \sin \theta_0 \cos \phi_0 \hat{\mathbf{F}}_x + \sin \theta_0 \sin \phi_0 \hat{\mathbf{F}}_y + \cos \theta_0 \hat{\mathbf{F}}_z$$

and $\hat{\mathbf{j}}$ is defined to have no $\hat{\mathbf{F}}_z$ component, while $\hat{\mathbf{i}}$, $\hat{\mathbf{j}}$, and $\hat{\mathbf{k}}$ must be orthonormal. The second two equations follow from expressing $(\hat{\mathbf{F}}_x, \hat{\mathbf{F}}_y, \hat{\mathbf{F}}_z)$ in terms of $(\hat{\mathbf{i}}, \hat{\mathbf{j}}, \hat{\mathbf{k}})$ and looking at the expansion of an arbitrary vector in the two bases. Substituting these relations into equation (5), we find

$$\begin{aligned} \hat{\mathbf{T}} = & \frac{r_0^2}{2 d_0^2} \sum_i v_i^2 \int \int_{S_i} \left(1 - \frac{2\Lambda d}{d_0} \right) \left[\hat{\mathbf{F}}_x (\beta \gamma_0 - \gamma \beta_0) \right. \\ & \left. + \hat{\mathbf{F}}_y (\gamma \alpha_0 - \alpha \gamma_0) + \hat{\mathbf{F}}_z (\alpha \beta_0 - \beta \alpha_0) \right] \frac{dr(0')/d(0')}{\sin \theta'} \sin \theta \, d\theta \, d\phi \quad . \end{aligned} \quad (6)$$

where $\alpha = \sin \theta \cos \phi$, $\beta = \sin \theta \sin \phi$, and $\gamma = \cos \theta$ and similarly for α_0 , β_0 , γ_0 . This is the basic equation we will use in all further calculations. All that needs to be done is to take an expression for Λd and $dr(0')/d(0')$ and calculate the integrals. Also note that $\hat{\mathbf{T}} \cdot \hat{\mathbf{k}} = 0$. The important quantity in the expression is $dr(0')/d(0')$, which determines the magnitude of the torques. This completes the derivation of the basic torque equation. The remainder of the report is devoted to evaluating the equation.

III. EXPANSION OF THE ROTOR SHAPE IN HARMONICS

The basic integral in equation (6) has been evaluated at great length by Honeywell [1] for hexahedral electrodes. This has been done by expanding Δd and $dr(\theta')/d\theta'$ in a Fourier cosine series and calculating the integral separately for each harmonic. The results of this will be discussed in Section IV, but here we wish to discuss the convergence of such a series. To do this we have taken the latest roundness measurements of the best available rotors by Rank-Taylor-Hobson (December 20, 1976). These measurements are taken over three great circles on the rotor; and, since we are assuming azimuthal symmetry, we need only half of each great circle. The three curves we have selected are shown in Figures 1, 2, and 3, which give Δr as a function of polar angle θ . While some improvement may occur due to spin averaging (see Section XI), we believe this is a reasonable place to start in evaluating the harmonics for realistic rotors.

Figures 4, 5, and 6, show the Fourier coefficients for the shapes given in Figures 1, 2, and 3, respectively. These have been obtained numerically from the actual assumed shapes. (The first harmonic has no significance for these calculations.) These curves show that we do get convergence, but it may require up to 20 harmonics depending on the scale of the irregularities in the rotor. For example, in Figure 3 more harmonics are required because of the sharpness of the bumps. In fact, there is an inverse relationship between the number of harmonics required and the smallest angular scale on which the irregularities occur. A rotor with very sharp bumps will require many harmonics to faithfully approximate its shape. The contribution to the integral in equation (6) from $dr(\theta')/d\theta'$ is proportional to $n\sin(n\theta)$ for the n th harmonic, so we have the possibility of increasing contributions to the torque as a result of increasingly higher harmonics. In fact, if Reference 1 is studied, it will be found that for the higher harmonics the number of terms in each torque expression actually increases with harmonic number, as do the coefficients of each term.

These considerations illustrate the basic problem with this type of calculation. It appears that contributions resulting from higher harmonics will be significant when added up, but it becomes extremely tedious to calculate equation (6) for the higher harmonics. This is only feasible up to about the sixth harmonic and is extremely difficult even up to this level, as a perusal of Reference 1 will show. The only way out of this dilemma appears to be the method we use in Section V, where we evaluate equation (6) numerically for some actual rotor shapes.

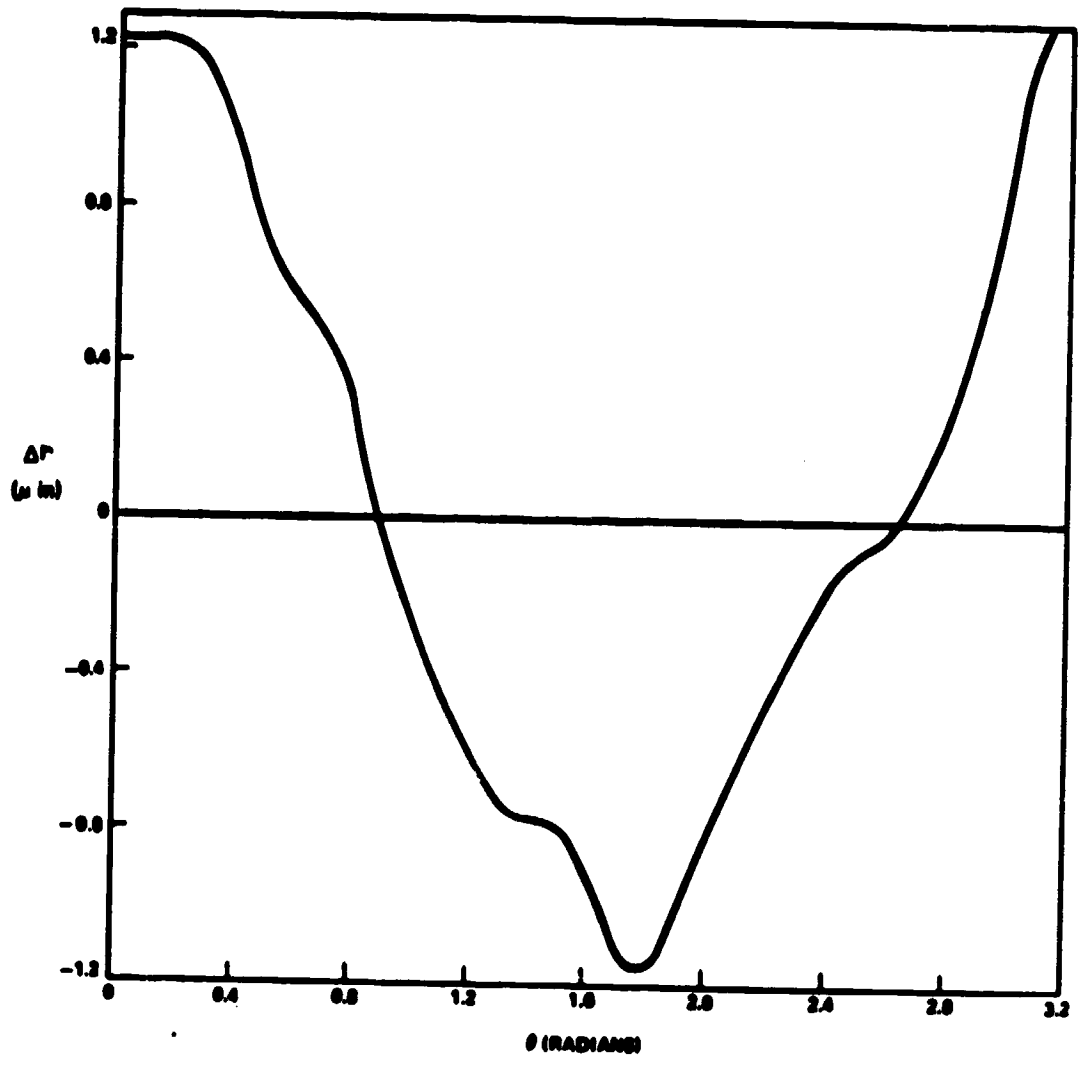


Figure 1. Deviation from sphericity. Case 1.

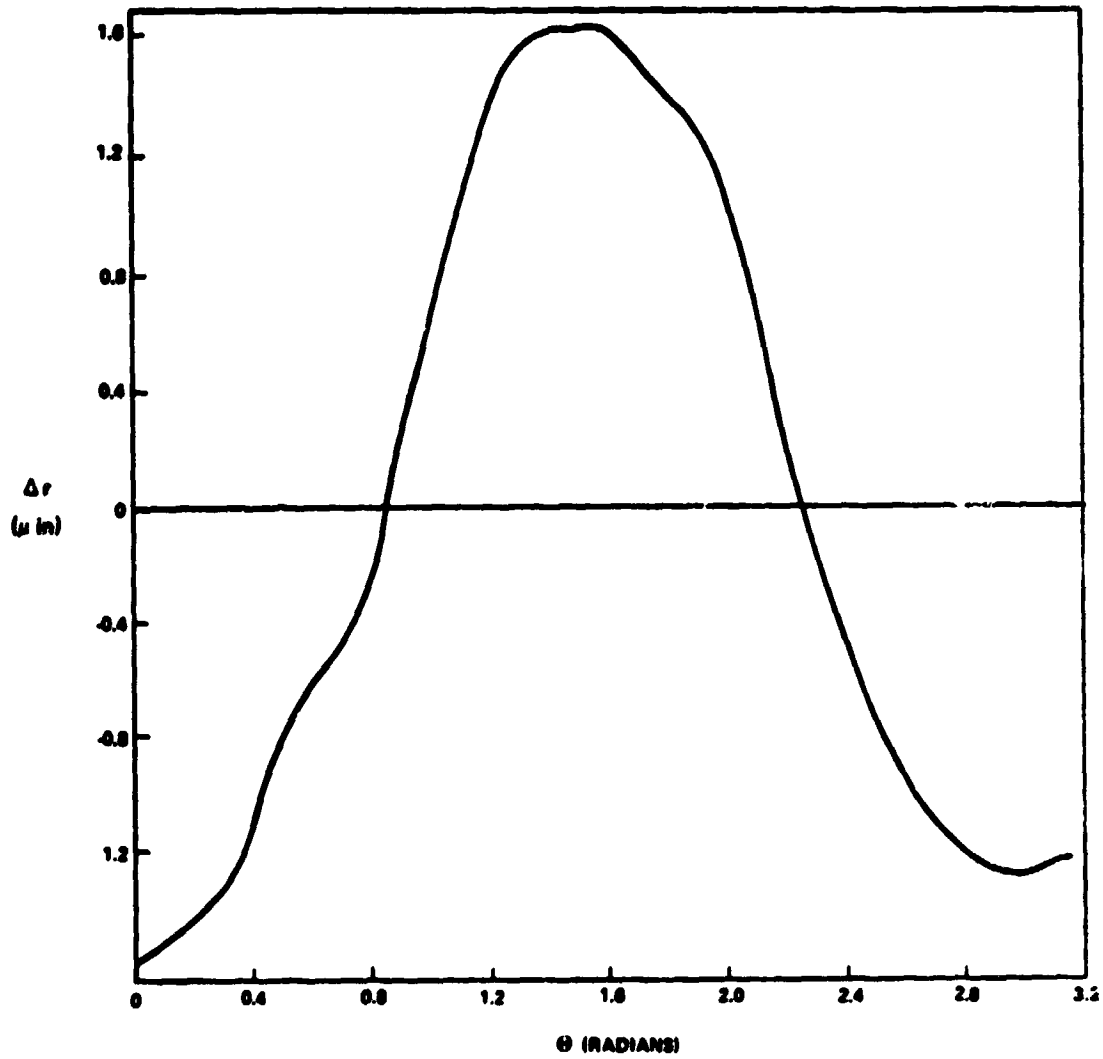


Figure 2. Deviation from sphericity, Case II.

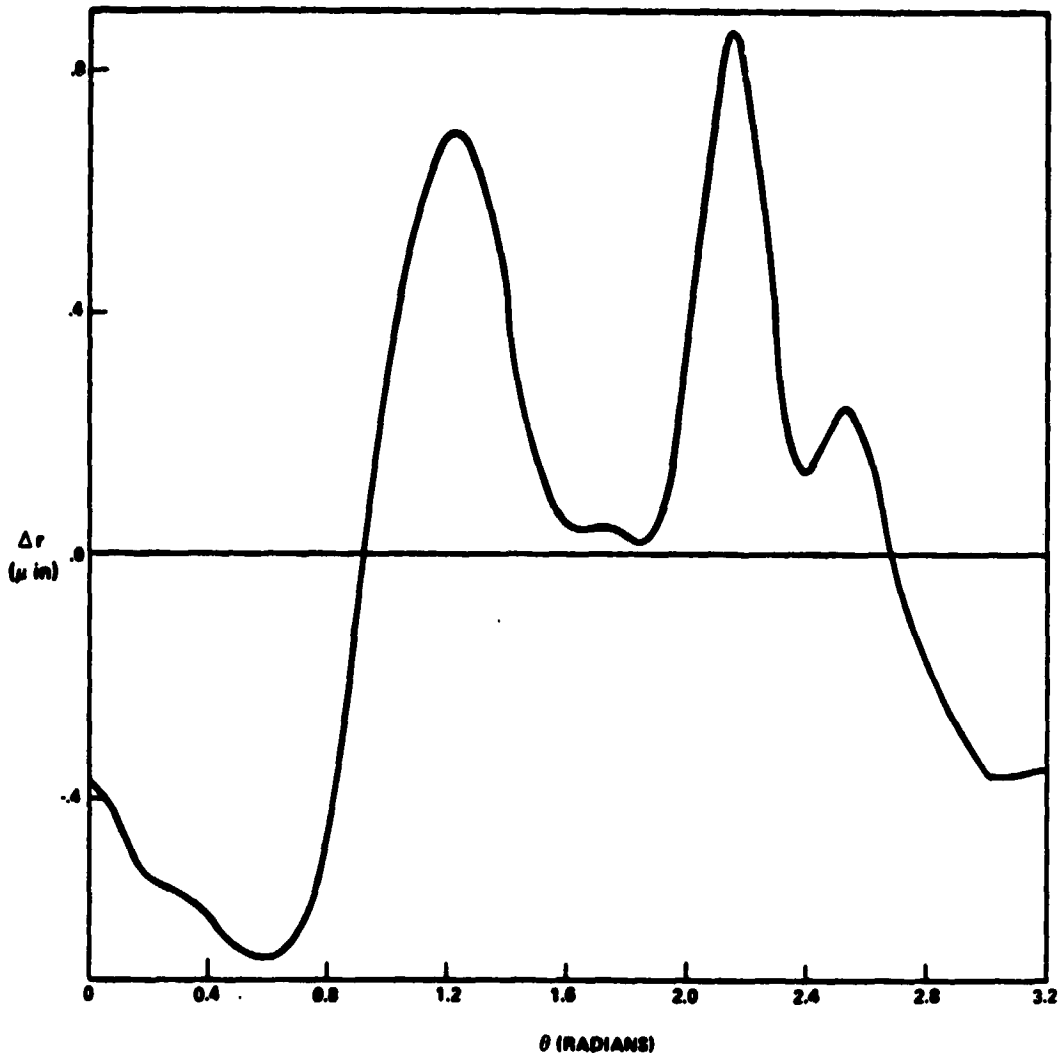


Figure 3. Deviation from sphericity, Case III.

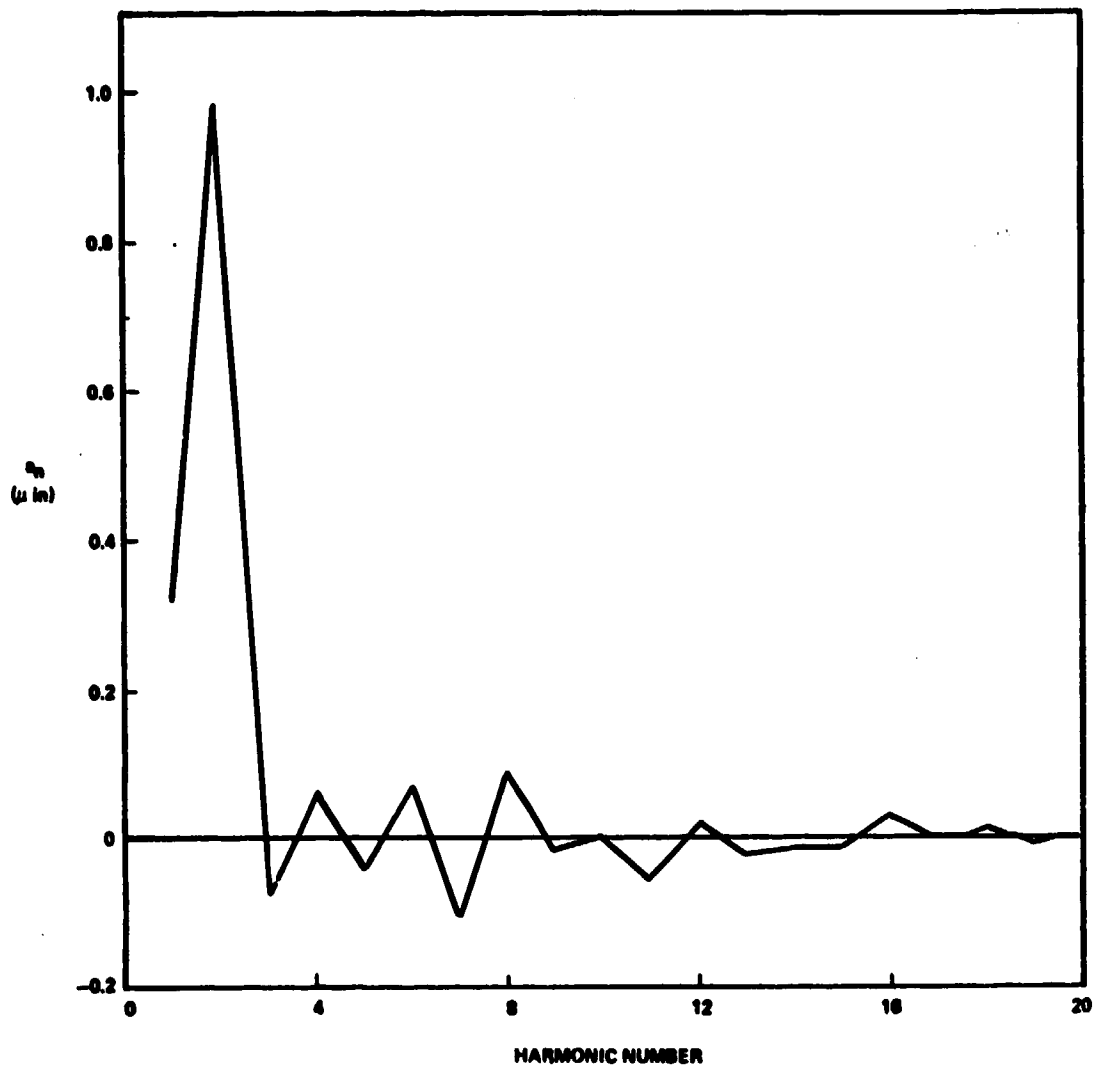


Figure 4. Size of harmonics, Case I.

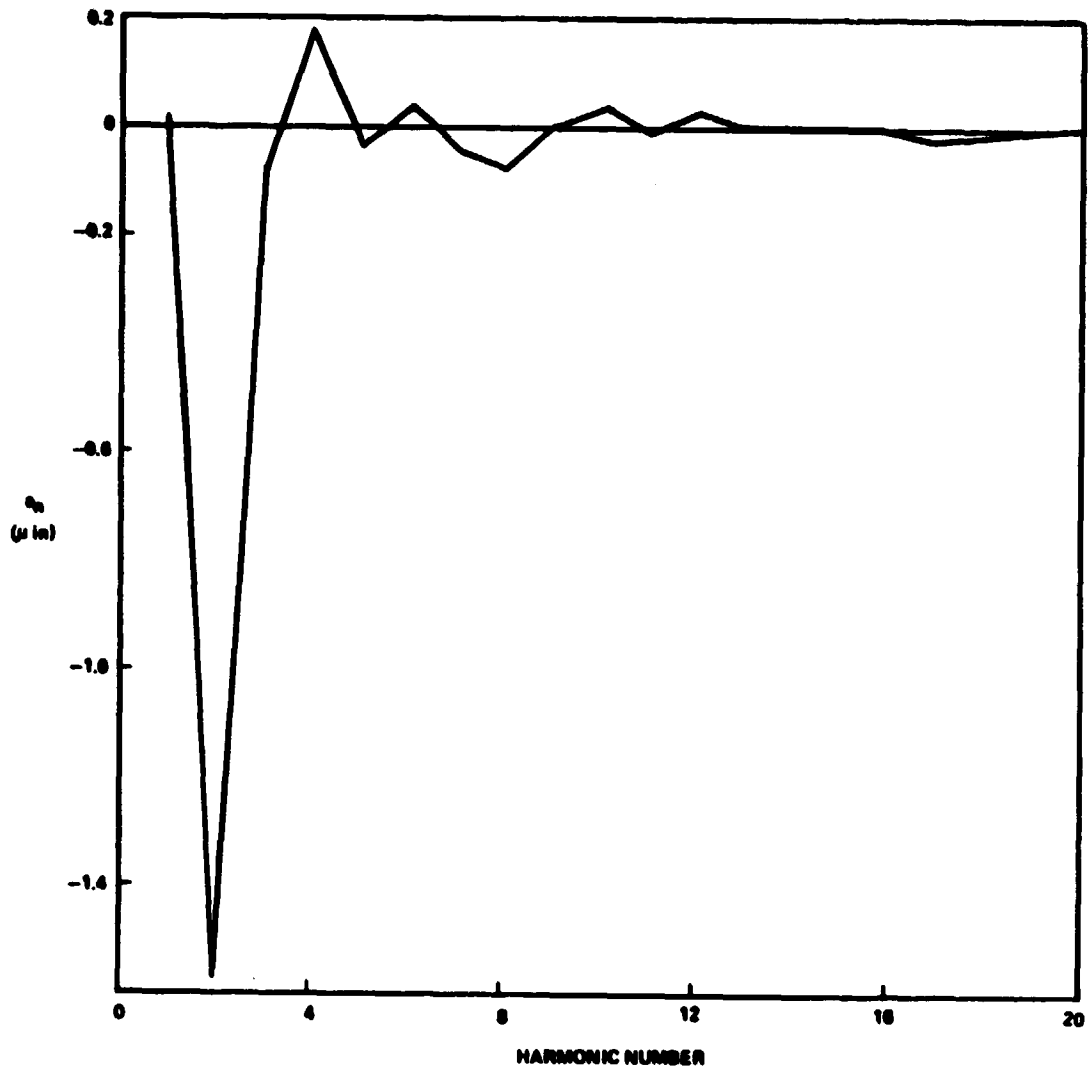


Figure 5. Size of harmonics, Case II.

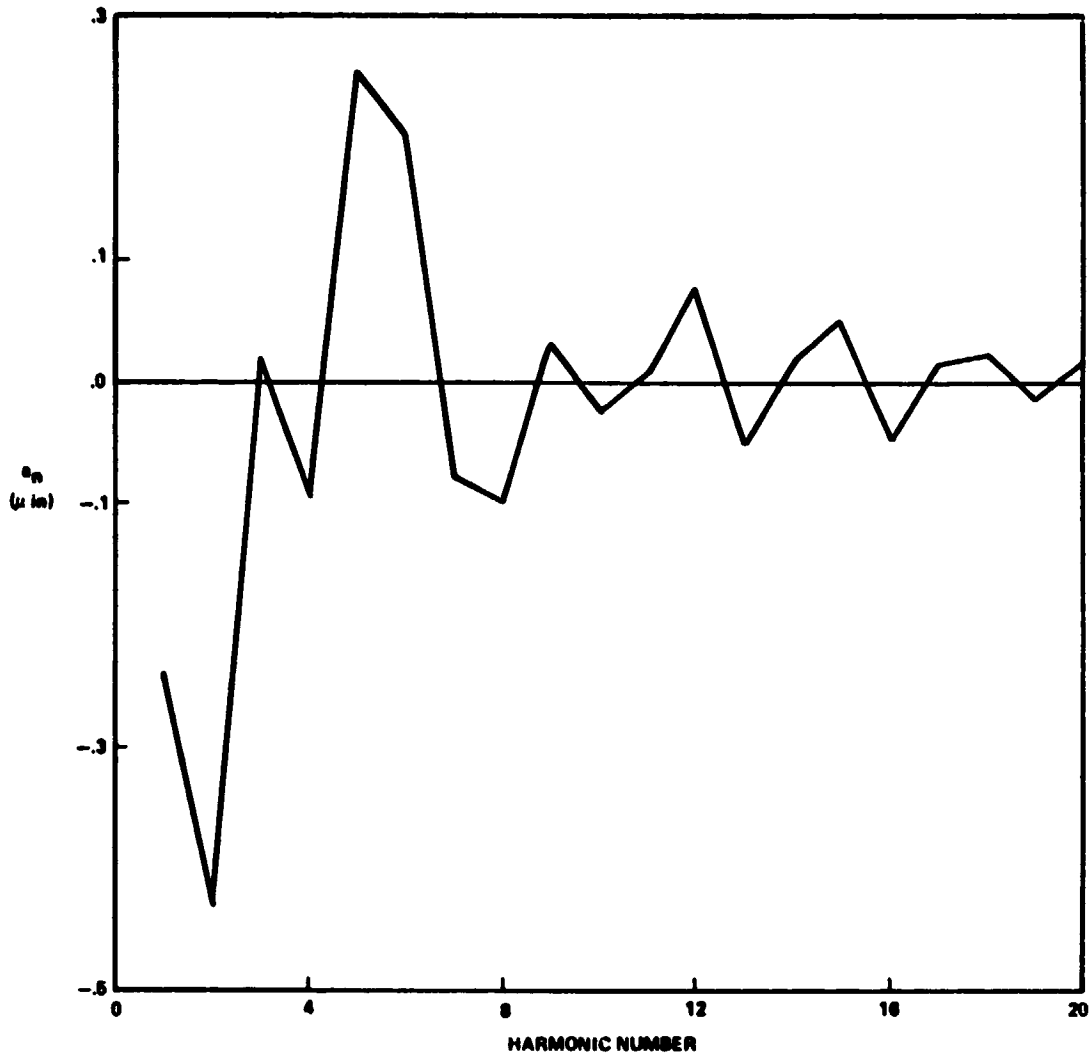


Figure 6. Size of harmonics, Case III.

IV. TORQUES IN TERMS OF HARMONICS

The method used to evaluate equation (6) is to expand $dr(\theta')/d\theta'$ and Δd in a Fourier series of the form

$$\Delta r = \sum_{n=2}^{\infty} a_n \cos(n\theta')$$

from which $dr(\theta')/d\theta'$ is obtained by differentiation, and the part of Δd due to rotor nonsphericity is obtained by $\Delta d = -\Delta r$. The torques due to just the $dr(\theta')/d\theta'$ term ($\Delta d = 0$) are known as primary torques. We have calculated these for circular electrodes up to the fifth harmonic; the results are shown in Table 1. The y and z components of T are obtained by suitable permutation of α_0 , β_0 , γ_0 and the P_i 's and M_i 's [1].

Honeywell has calculated these torques up to the sixth harmonic for hexahedral electrodes. We have developed a computer program to evaluate our expressions to see the angular behavior of the torques. This is necessary because heretofore the torques have been estimated from expressions valid only near the z-axis, and it is of interest to see how these torques behave for arbitrary orientations. Also, with our computer calculation we can compare the actual magnitudes of the second versus fourth and third versus fifth harmonics to see if convergence is occurring. Figures 7 through 10 show the relative magnitude of the torques for the second through the fifth harmonic in arbitrary units for typical values of the harmonic coefficients. The second harmonic is small because we have assumed equal preloads. It is clear that the fourth and fifth harmonics produce torques of the same order of magnitude as the second and third. A large number of calculations that are not shown here bear this out. This is also obvious from the inspection of Table 1. The expressions in Table 2 are computed from general expressions for the torque as in Table 1 by specializing the expressions to the case $\gamma_0 \approx 1$, $\alpha_0 \ll 1$, $\beta_0 \ll 1$ and defining $\Omega = T/I\omega$, where T is the magnitude of the torque, $I = 2/5 mr^2$ is the moment of inertia of the rotor and $\omega = v/r$ is the angular velocity of the rotor. The connection between the M's and P's in Table 1 and the acceleration f and preload h are derived as follows. From equation (1) we have for circular electrodes that the force on the rotor is

$$\vec{F} = m \sin^2 \theta_1 (M_x \hat{F}_x + M_y \hat{F}_y + M_z \hat{F}_z) \quad ; \quad (7)$$

this determines the components of the acceleration as

TABLE 1

$$\begin{aligned}
 T_x = & 2.727 a_2 (P_z - P_y) \beta_o \gamma_o + a_3 \left\{ 7.078 (\beta_o \gamma_o^2 M_z \right. \\
 & - \beta_o^2 \gamma_o M_y) + 0.5890 [(\beta_o^3 + \alpha_o^2 \beta_o) M_z - (\gamma_o^3 + \alpha_o^2 \gamma_o) M_y] \\
 & + 2.356 (\gamma_o M_y - \beta_o M_z) \left. \right\} + a_4 \left\{ \beta_o \gamma_o^3 (16.37 P_z + 3.74 P_y) \right. \\
 & - \beta_o^3 \gamma_o (3.740 P_z + 16.37 P_y) + 3.740 \alpha_o^2 \beta_o \gamma_o (P_y - P_z) \\
 & + 10.91 \beta_o \gamma_o (P_y - P_z) \left. \right\} + 10 \pi a_5 \left\{ 0.5625 \beta_o^2 \gamma_o^2 (\beta_o M_z \right. \\
 & - \gamma_o M_y) + 0.5625 \alpha_o^2 \beta_o \gamma_o (\gamma_o M_z - \beta_o M_y) \\
 & + 1.1273 \beta_o \gamma_o (\gamma_o^3 M_z - \beta_o^3 M_y) + 0.03125 \alpha_o^2 (\beta_o^3 M_z \\
 & - \gamma_o^3 M_y) + 0.01562 [\beta_o (\beta_o^4 + \alpha_o^4) M_z - \gamma_o (\gamma_o^4 \\
 & + \alpha_o^4) M_y] + 0.09375 [\gamma_o (\gamma_o^2 + \alpha_o^2) M_y - \beta_o (\beta_o^2 \\
 & + \alpha_o^2) M_z] + 1.1265 \beta_o \gamma_o (\beta_o M_y - \gamma_o M_z) \\
 & \left. + 0.125 (\beta_o M_z - \gamma_o M_y) \right\} .
 \end{aligned}$$

$$P_i = \frac{\epsilon_o r_o^2}{2 d_o^2} ((V_{i+}^2 + V_{i-}^2))$$

$$M_i = \frac{\epsilon_o r_o^2}{2 d_o^2} ((V_{i+}^2 - V_{i-}^2))$$

$\theta_1 = 30^\circ =$ electrode half angle

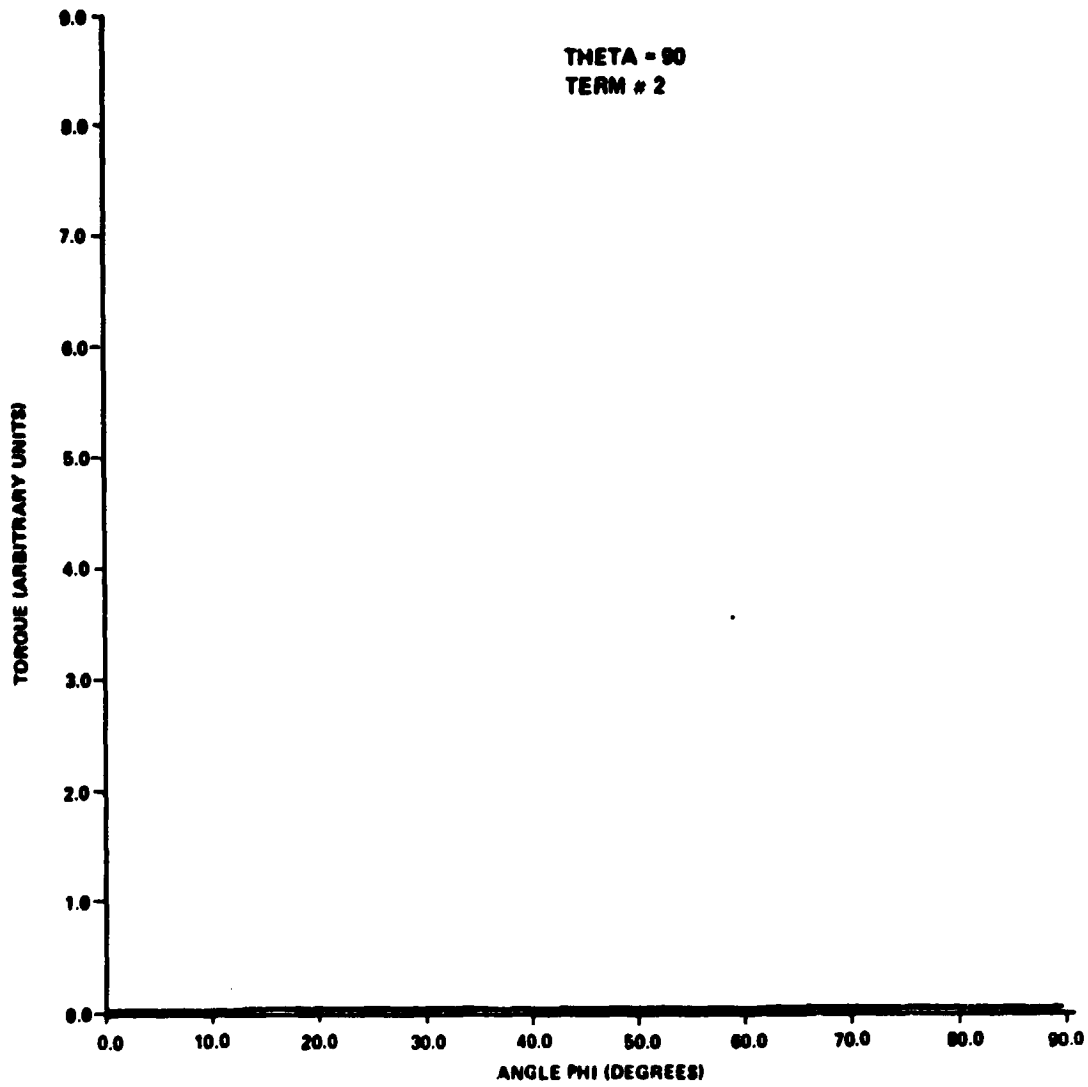


Figure 7. Second harmonic torque versus angle.

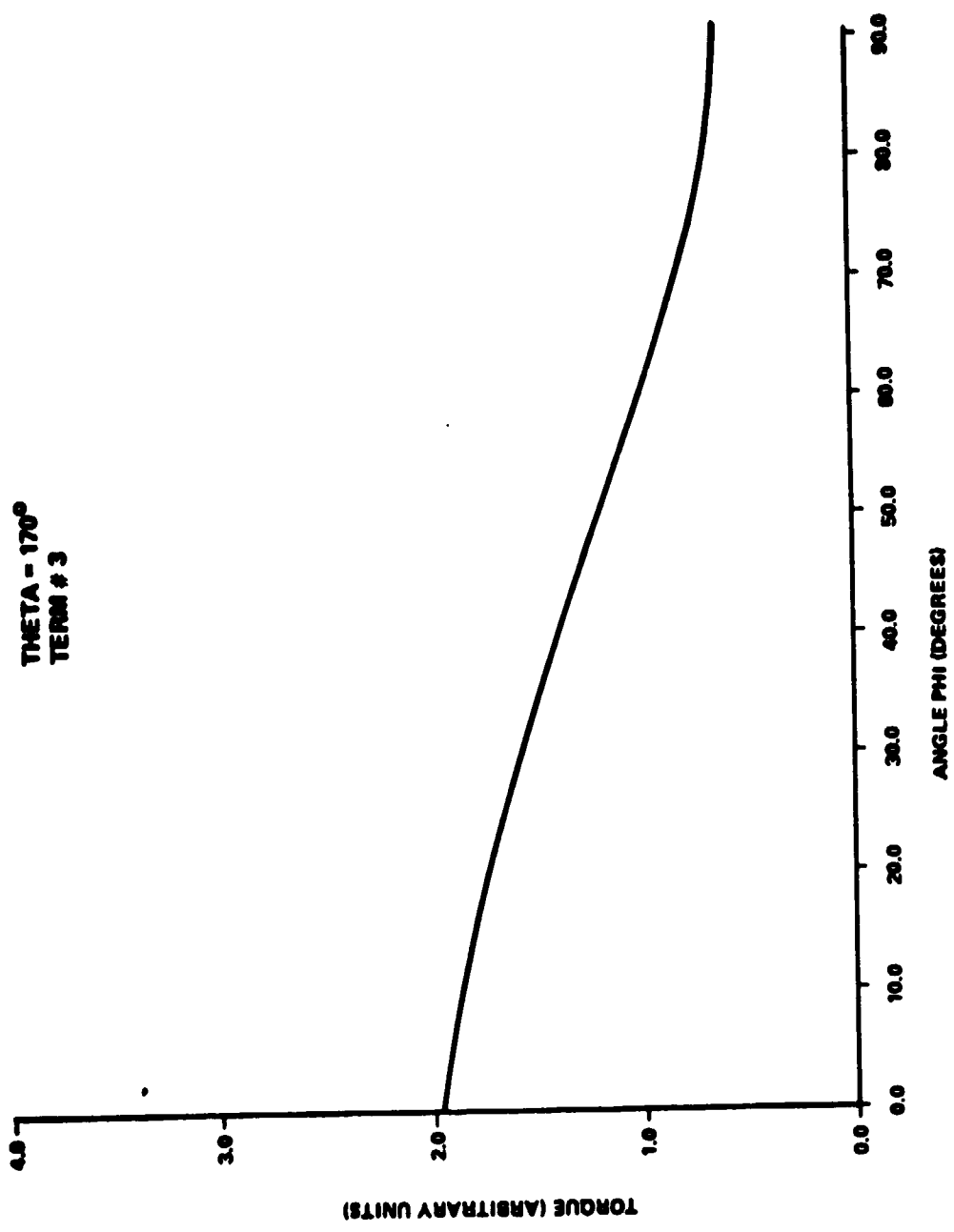


Figure 8. Third harmonic torque versus angle.

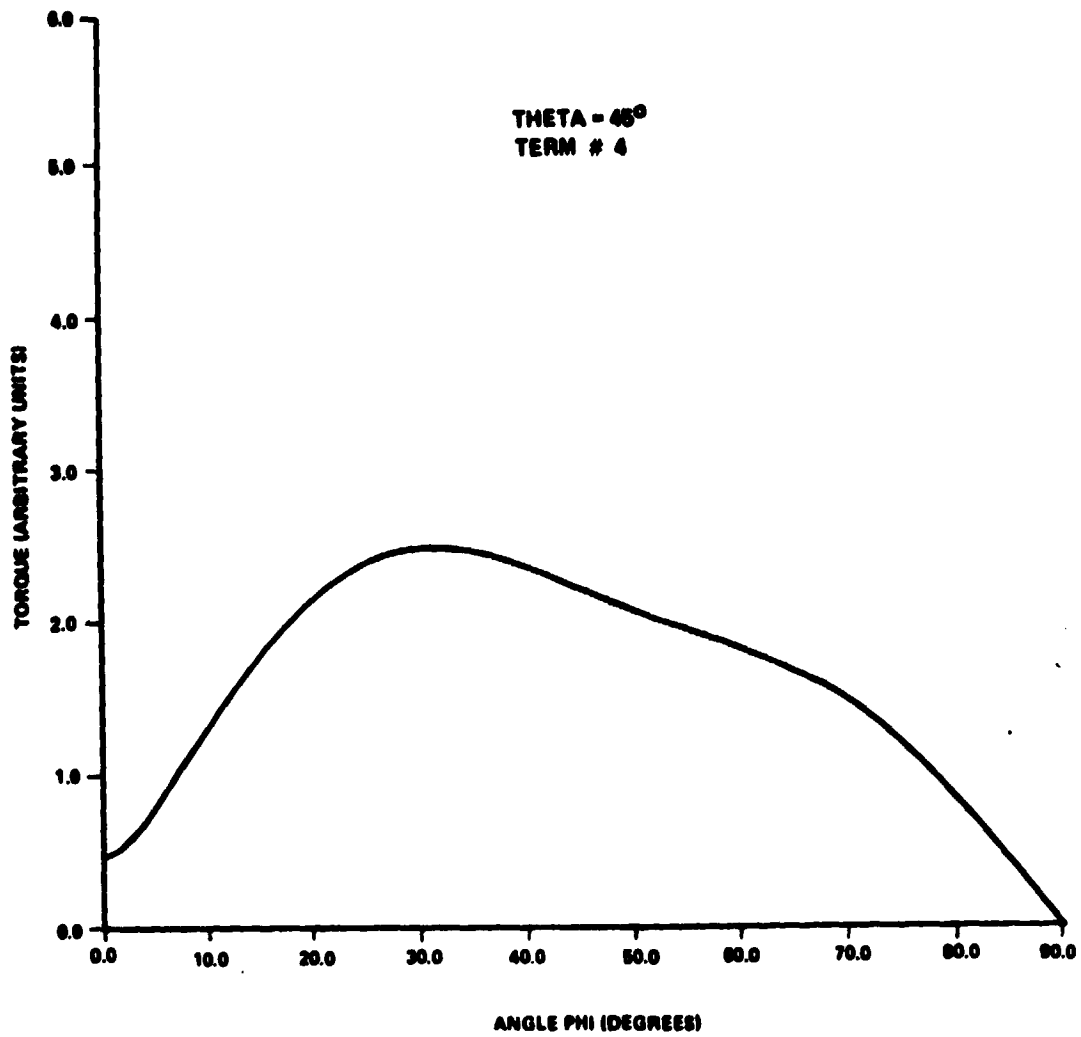


Figure 9. Fourth harmonic torque versus angle.

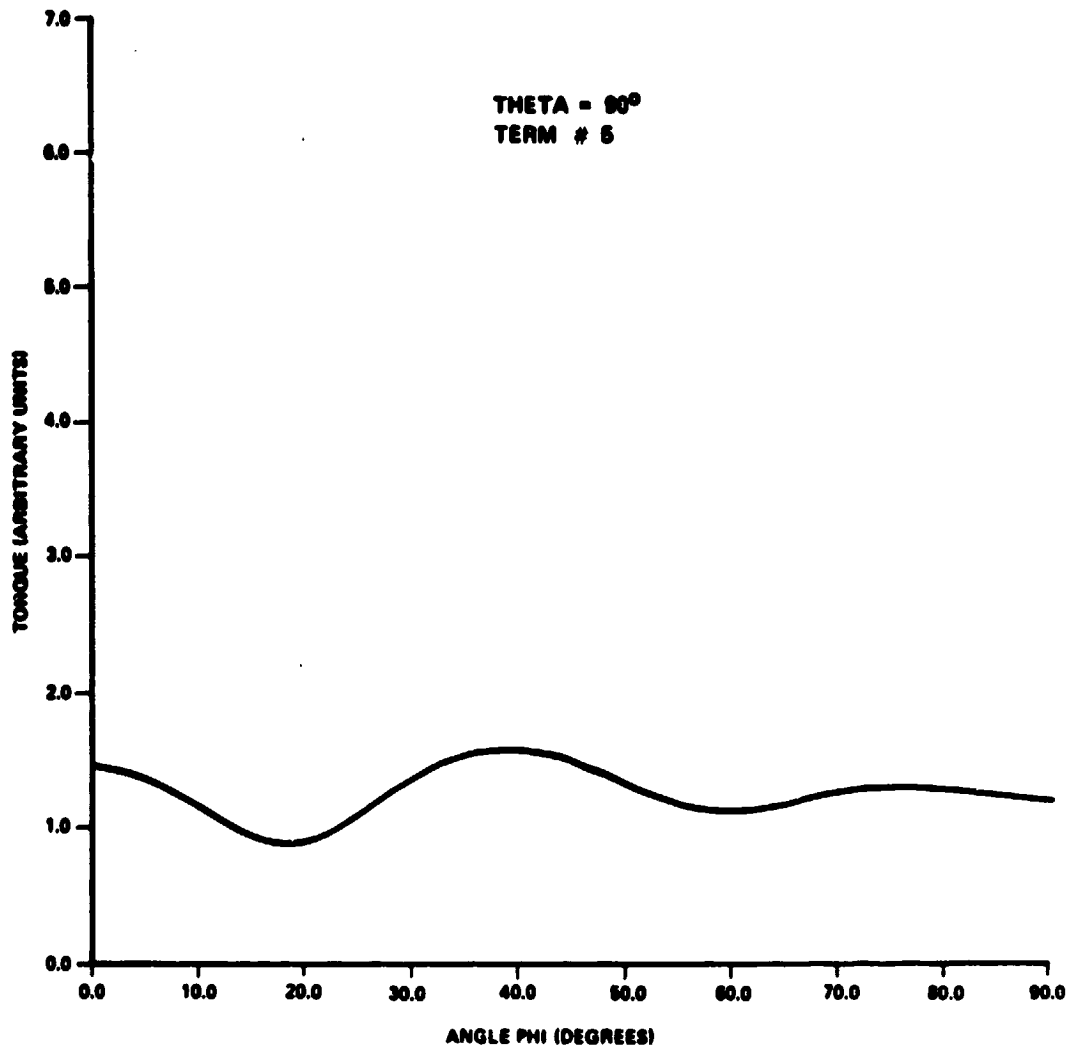


Figure 10. Fifth harmonic torque versus angle.

TABLE 2

<u>Drift Rates</u>	<u>Second Harmonic</u>	<u>Third Harmonic</u>
Aligned	0	$\frac{15}{2} (\cos^2 \theta_1 - \frac{1}{5}) \left(\frac{a_3}{r_0}\right) \left(\frac{f}{V}\right)$
Misaligned	$5 \cos^2 \theta_1 \left(\frac{a_2}{r_0}\right) \left(\frac{h}{V}\right) \left(h + \frac{f^2}{h}\right)$	$\frac{15}{2} (4 \cos^2 \theta_1 - 1) \left(\frac{a_3}{r_0}\right) \left(\frac{f}{V}\right) e$
Miscentered	$5 \sin^2 \theta_1 \left(\frac{a_2}{r_0}\right) \left(\frac{t}{d_0}\right) \left(\frac{f}{V}\right)$	$\frac{3}{2} \left(\frac{2 - \cos^4 \theta_1 (7 \cos^4 \theta_1 - 10 \cos^2 \theta_1 + 5)}{\sin^2 \theta_1} \right) \left(\frac{a_3}{r_0}\right) \left(\frac{t}{d_0}\right) \left(\frac{h}{V}\right) \left(1 + \frac{f^2}{h}\right)$

θ_1 = electrode half angle

r_0 = rotor radius

V = peripheral velocity

h = prebend

h = difference in prebend for different axes

f = acceleration

t = miscentering

d_0 = nominal rotor electrode gap

θ = misalignment angle

$$f_x = \frac{\pi \sin^2 \theta_1}{m} M_x .$$

The expression in Table 2 for the aligned third harmonic then agrees with that of Table 1 except for the $-1/5$, which represents the displacement of the center of mass for a pear-shaped rotor of this type. Similarly, for the misaligned third harmonic, the terms in Tables 1 and 2 agree if we take $\beta_0 = 0$ and neglect α_0^2 and β_0^2 . This brings out the fact that the expressions in Table 2 are only good for $\gamma_0 \sim 1$ (gimbaled gyro) and shows why it is necessary to write a computer program to evaluate these torques for the nongimbaled case. This is described in Section V for all the harmonics.

The preload h_i is defined here as the acceleration that will drive the voltage on one of the i th electrodes to zero and thus lose the suspension. (This definition differs from that of Reference 1.) For a linear suspension system we have $V_{i+} + V_{i-} = V_{i0} = \text{constant}$, so from equation (7)

$$mh_i = \frac{r_0^2}{2 d_0^2} (V_{i0}^2) (\pi \sin^2 \theta_1) .$$

Using the identity

$$\begin{aligned} (V_{i-}^2 + V_{i+}^2) &= \frac{1}{2} \left[(V_{i+} + V_{i-})^2 + \frac{(V_{i+}^2 - V_{i-}^2)^2}{(V_{i+} + V_{i-})^2} \right] \\ &= \frac{V_{i0}^2}{2} \left[1 + \frac{(V_{i+}^2 - V_{i-}^2)^2}{V_{i0}^4} \right] \end{aligned}$$

and multiplying by $r_0^2 / 2 d_0^2$, we obtain

$$P_i = \frac{m}{2 \pi \sin^2 \theta_1} \left[h_i + \frac{f_i^2}{h_i} \right] . \quad (8)$$

This is the basic equation connecting P_1 with h_1 and f_1 . The preloads h_1 are adjusted to be larger than the maximum acceleration expected in a given environment. The misaligned second harmonic in Table 2 is seen to agree with Table 1 if β_0 is again identified with β and ϵ is the difference in preloads for different axes.

Comparing these expressions with Reference 2 indicates that there are terms present for the aligned and miscentered third harmonic that are not included in Reference 2. These two terms put more severe restrictions on f and h than have previously been indicated. We postpone generating actual numerical tolerances until Section VI and refer to Reference 3, where numerical values for the parameters in Table 2 are given which allow the reduction of Ω to $\Omega_0 = 1.6 \times 10^{-16}$ rad/sec = 0.001 arc sec/yr, the accuracy necessary for a 2 percent measurement of the Lense Thirring effect.

Tables 3 and 4 contain miscentering torques for the second and third harmonics in terms of arbitrary electrode angle θ_1 . The corresponding expressions in Table 2 are obtained for the case $\gamma_0 = 1$ as before. These expressions illustrate the rapid increase in complexity for higher harmonics.

It is important to realize that the simplified expressions in Table 2 which have been used in previous drift estimates are only valid for near alignment of the rotor spin with the electrode axis. When this is not the case, the expressions in terms of harmonics become extremely tedious to evaluate for the higher harmonics, and it is best to resort to numerical integration of equation (6), as in Section V. The planned orientation for the final gyro experiment is not the gimballed case but the case where the spin axis is midway between two electrodes. Thus, the expressions in Table 2 are not really relevant for this orientation, and what we really need is the case $\gamma_0 = \alpha_0 = 1/\sqrt{2}$. This is difficult to evaluate for all the terms in Table 1, but we immediately realize that the alignment factor θ for the second harmonic is no longer applicable. This is a very important point and increases the corresponding drifts by at least two orders of magnitude. This point is discussed further in Sections VI and VII.

TABLE 3. SECOND HARMONIC MISCENTERING TORQUE (CIRCULAR ELECTRODES)

$$\begin{aligned}
 \frac{\dot{r}_2}{a_2} \Big|_{x_c} &= \frac{x_c}{d_0} \left[\hat{F}_x \left\{ (2 - \sin^4 \theta_1) (\alpha_0 (\beta_0 M_z - \gamma_0 M_y)) \right\} + \hat{F}_y \left\{ (2 - \sin^4 \theta_1) (\beta_0 \gamma_0 M_y) \right. \right. \\
 &\quad \left. \left. - (\alpha_0^2 - \gamma_0^2) M_x \right\} + 2 - \sin^4 \theta_1 (1 + 2 \cot^4 \theta_1) (\alpha_0 \gamma_0 M_x) \right] \\
 &\quad + \hat{F}_z \left\{ (2 - \sin^4 \theta_1) [-\beta_0 \gamma_0 M_z - (\alpha_0^2 - \gamma_0^2) M_y] - (2 - \sin^4 \theta_1) (1 \right. \\
 &\quad \left. + 2 \cot^4 \theta_1) (\beta_0 \alpha_0 M_x) \right\}
 \end{aligned}
 \tag{1}$$

x_c = miscentering error in x direction

TABLE 4. THIRD HARMONIC MISCENTERING TORQUE
(CIRCULAR ELECTRODES)

$$\begin{aligned} \frac{\dot{T}_3}{24 a_3} \Big|_{x_c} = & \frac{x_c}{d_o} \left\{ \hat{F}_x \left[\alpha_o \beta_o \gamma_o \left(-\frac{5}{2} \Lambda_2 - 2 \Lambda_1 \right) (P_z - P_y) \right] \right. \\ & + \hat{F}_y \left[\alpha_o^2 \gamma_o \left\{ P_x \left(2 \Lambda_2 - 2 \Lambda_1 + 2 \pi \frac{(1 - \cos^5 \theta_1)}{5} \right) \right. \right. \\ & + P_y \left(\frac{\Lambda_2}{4} \right) + P_z \left(\frac{11\Lambda_2}{4} - 2 \Lambda_1 \right) \left. \right\} + \beta_o^2 \gamma_o \left\{ (P_x \right. \\ & + P_y) (\Lambda_1 - \Lambda_2) + P_z \left(\frac{\Lambda_2}{4} \right) \left. \right\} + \gamma_o^3 \left\{ (P_x + P_z) (\Lambda_1 \right. \\ & - \Lambda_2) + P_y \left(\frac{\Lambda_2}{4} \right) \left. \right\} - \gamma_o \left\{ (P_y + P_z) \left(\frac{\Lambda_1}{4} \right) \right. \\ & + P_x \left(\pi \frac{(1 - \cos^3 \theta_1)}{6} \right) \left. \right\} \left. \right] - \hat{F}_z \left[\alpha_o^2 \beta_o \left\{ P_x \left(2 \Lambda_2 \right. \right. \right. \\ & - 2 \Lambda_1 + \frac{(1 - \cos^5 \theta_1)}{2} \left. \right\} + P_z \left(\frac{\Lambda_2}{4} \right) - P_y \left(\frac{11\Lambda_2}{4} - 2 \Lambda_1 \right) \left. \right\} \\ & + \beta_o^3 \left\{ (P_x + P_y) (\Lambda_1 - \Lambda_2) + P_z \left(\frac{\Lambda_2}{4} \right) \right\} \\ & + \beta_o \gamma_o^2 \left\{ (P_x + P_y) (\Lambda_1 - \Lambda_2) + P_y \left(\frac{\Lambda_2}{4} \right) \right\} \\ & \left. - \beta_o \left\{ (P_y + P_z) \left(\frac{\Lambda_1}{4} \right) + P_x \left(\pi \frac{(1 - \cos^3 \theta_1)}{6} \right) \right\} \right] \left. \right\} \end{aligned}$$

$$\Lambda_1 = \pi \int_0^{\theta_1} \sin^3 \theta d\theta$$

$$\Lambda_2 = \pi \int_0^{\theta_1} \sin^5 \theta d\theta$$

V. EXACT NUMERICAL CALCULATION OF TORQUES

It is possible to evaluate equation (6) for arbitrary rotor spin orientation by doing the integrals numerically. To do this we use the substitutions in Reference 1 to include all the electrodes; that is:

z- electrode	$\alpha \rightarrow -\alpha, \gamma \rightarrow -\gamma$
x+ electrode	$\alpha \rightarrow \gamma, \gamma \rightarrow -\alpha$
x- electrode	$\alpha \rightarrow -\gamma, \beta \rightarrow -\beta, \gamma \rightarrow -\alpha$
y+ electrode	$\alpha \rightarrow -\beta, \beta \rightarrow \gamma, \gamma \rightarrow -\alpha$
y- electrode	$\alpha \rightarrow \beta, \beta \rightarrow -\gamma, \gamma \rightarrow -\alpha$

One notices then that permuting $\alpha, \beta,$ and γ is equivalent to permuting $\alpha_0, \beta_0,$ and γ_0 in the expression for θ' and at the same time permuting the three basic integrals given by

$$I_1(\alpha_0, \beta_0, \gamma_0) = \int_0^{2\pi} d\phi \int_0^1 \sin \theta d\theta \left[\alpha \frac{dr(\theta')/d\theta'}{\sin \theta'} \right]$$

$$I_2(\alpha_0, \beta_0, \gamma_0) = \int_0^{2\pi} d\phi \int_0^1 \sin \theta d\theta \left[\beta \frac{dr(\theta')/d\theta'}{\sin \theta'} \right]$$

$$I_3(\alpha_0, \beta_0, \gamma_0) = \int_0^{2\pi} d\phi \int_0^1 \sin \theta d\theta \left[\gamma \frac{dr(\theta')/d\theta'}{\sin \theta'} \right]$$

$$\cos \theta' = \alpha\alpha_0 + \beta\beta_0 + \gamma\gamma_0$$

$$\alpha = \sin \theta \cos \phi$$

$$\beta = \sin \theta \sin \phi$$

$$\gamma = \cos \theta$$

Thus, it is possible to express equation (6) in terms of these three basic integrals with the arguments permuted in the appropriate fashion. The end result of this is as follows (where we have neglected the Δ/d term):

$$\begin{aligned}
 T_x = \frac{c_o r_o^2}{2 d_o^2} & \left\{ \gamma_o [V_{z+}^2 I_2(\alpha_o, \beta_o, \gamma_o) + V_{z-}^2 I_2(-\alpha_o, \beta_o, -\gamma_o)] \right. \\
 & + V_{x+}^2 I_2(-\gamma_o, \beta_o, \alpha_o) - V_{x-}^2 I_2(-\gamma_o, -\beta_o, -\alpha_o) + V_{y+}^2 I_3(-\gamma_o, -\alpha_o, \beta_o) \\
 & - V_{y-}^2 I_3(-\gamma_o, \alpha_o, -\beta_o)] + \beta_o [V_{z+}^2 I_3(\alpha_o, \beta_o, \gamma_o) \\
 & + V_{z-}^2 I_3(-\alpha_o, \beta_o, -\gamma_o)] + V_{x+}^2 I_1(-\gamma_o, \beta_o, \alpha_o) + V_{x-}^2 I_1(-\gamma_o, -\beta_o, -\alpha_o) \\
 & \left. + V_{y+}^2 I_1(-\gamma_o, -\alpha_o, \beta_o) + V_{y-}^2 I_1(-\gamma_o, \alpha_o, -\beta_o)] \right\} \\
 T_y = \frac{c_o r_o^2}{2 d_o^2} & \left\{ \alpha_o [V_{z+}^2 I_3(\alpha_o, \beta_o, \gamma_o) - V_{z-}^2 I_3(-\alpha_o, \beta_o, -\gamma_o)] \right. \\
 & - V_{x+}^2 I_1(-\gamma_o, \beta_o, \alpha_o) - V_{x-}^2 I_1(-\gamma_o, -\beta_o, -\alpha_o) - V_{y-}^2 I_1(-\gamma_o, -\alpha_o, \beta_o) \\
 & - V_{y+}^2 I_1(-\gamma_o, \alpha_o, -\beta_o)] + \gamma_o [V_{z+}^2 I_1(\alpha_o, \beta_o, \gamma_o) \\
 & + V_{z-}^2 I_1(-\alpha_o, \beta_o, -\gamma_o)] - V_{x+}^2 I_3(-\gamma_o, \beta_o, \alpha_o) + V_{x-}^2 I_3(-\gamma_o, -\beta_o, -\alpha_o) \\
 & \left. + V_{y+}^2 I_2(-\gamma_o, -\alpha_o, \beta_o) - V_{y-}^2 I_2(-\gamma_o, \alpha_o, -\beta_o)] \right\}
 \end{aligned}$$

$$\begin{aligned}
T_z = \frac{\epsilon_0 r_0^2}{2 d_0^2} \left\{ \beta_0 [V_{z+}^2 I_1(\alpha_0, \beta_0, \gamma_0) - V_{z-}^2 I_1(-\alpha_0, \beta_0, -\gamma_0)] \right. \\
+ V_{x+}^2 I_3(-\gamma_0, \beta_0, \alpha_0) - V_{x-}^2 I_3(-\gamma_0, -\beta_0, -\alpha_0) - V_{y+}^2 I_2(-\gamma_0, -\alpha_0, \beta_0) \\
+ V_{y-}^2 I_2(-\gamma_0, \alpha_0, -\beta_0)] + \alpha_0 [-V_{z+}^2 I_2(\alpha_0, \beta_0, \gamma_0) \\
- V_{z-}^2 I_2(-\alpha_0, \beta_0, -\gamma_0) - V_{x+}^2 I_2(-\gamma_0, \beta_0, \alpha_0) + V_{x-}^2 I_2(-\gamma_0, -\beta_0, -\alpha_0) \\
\left. - V_{y+}^2 I_3(-\gamma_0, -\alpha_0, \beta_0) + V_{y-}^2 I_3(-\gamma_0, \alpha_0, -\beta_0)] \right\} .
\end{aligned}$$

This is the final exact expression for the primary torques (with no $\Delta d/d_0$ terms) in terms of an arbitrary rotor shape $r(\theta')$, and it does not rely on a harmonic expansion. The V_i 's can be expressed in terms of f_i and h_i directly from equations (7) and (8) as

$$V_{i\pm}^2 = \frac{d_0^2}{\epsilon_0 r_0^2} \left[\pm f_i + \frac{1}{2} \left(h_i + \frac{f_i^2}{h_i} \right) \right] \frac{m}{\pi \sin^2 \theta_1} . \quad (9)$$

We have written a computer program (see Appendix) to evaluate these integrals numerically for an $r(\theta')$ which we can take directly from a roundness chart. The program does the double integrals using an 8-point Newton Coates quadrature formula with 97 divisions. It has been checked with the analytic expressions for the second and third harmonics in Table 1 and found to be accurate to four significant figures. The $r(\theta')$ is Fourier analyzed ($0 \leq \theta' \leq \pi$), and the Fourier cosine series coefficients up to the 20th are used to reconstruct $dr(\theta')/d\theta'$. Thus, we expect harmonics up to the 20th to be accounted for.

VI. NUMERICAL RESULTS

A number of computer runs were undertaken to establish the drift rates for various values of the parameters involved. The three sample rotors were used as previously described. To establish the preload dependence, a series of computations were made for a rotor orientation of $\theta_0 = 45^\circ$, $\phi_0 = 0^\circ$, where θ_0 is the angle from the electrode axis and ϕ_0 is the azimuthal angle.

The results are shown in Tables 5 through 8 for various levels of acceleration. The h's were taken to differ by 1 percent. The results indicate that the drifts are proportional to the preload for the lower values of f. The drifts indicate the general order of magnitude to be expected for arbitrary rotor orientation. The general level of drift was several hundred milliarc sec/yr for $h \sim 10^{-6}$ g.

TABLE 5. DRIFT RATES

($\theta_0 = 45^\circ$, $\phi_0 = 0^\circ$, $f \sim 10^{-10}$ g, $\Delta h = 0.01$ h)

h(g's)	Case I	Case II	Case III
	(milliarc sec/yr)		
10^{-6}	86.0	291.0	202.0
10^{-7}	8.6	29.1	20.4
10^{-8}	0.89	3.01	2.30

TABLE 6. DRIFT RATES

($\theta_0 = 45^\circ$, $\phi_0 = 0^\circ$, $f \sim 10^{-9}$ g, $\Delta h = 0.01$ h)

h(g's)	Case I	Case II	Case III
	(milliarc sec/yr)		
10^{-6}	86.0	291.0	204.0
10^{-7}	8.9	30.0	23.0
10^{-8}	2.5	8.3	8.5

TABLE 7. DRIFT RATES

($\theta_0 = 45^\circ$, $\phi_0 = 0^\circ$, $f \sim 10^{-8}$ g, $\Delta h = 0.01$ h)

h (g's)	Case I (milliarc sec/yr)	Case II	Case III
10^{-6}	89.0	300.0	210.0
10^{-7}	25.0	84.0	85.0
10^{-8}	150.0	505.0	370.0

TABLE 8. DRIFT RATES

($\theta_0 = 45^\circ$, $\phi_0 = 0^\circ$, $f \sim 10^{-7}$ g, $\Delta h = 0.01$ h)

h (g's)	Case I (milliarc sec/yr)	Case II	Case III
10^{-6}	254.0	839.0	850.0
10^{-7}	1497.0	5053.0	3705.0

Next the relative effect of the higher harmonics was investigated by running the program for each harmonic separately normalized to a harmonic coefficient of $a_n = 1$ μ in. One sees from Table 9 that the higher harmonics do not decrease in importance very quickly. Combining this with Figures 4, 5, and 6, we see that the a_n above the second do not drop off very quickly, so that the higher harmonics may be important and should be included in the calculation.

TABLE 9. DRIFT RATES ($f \sim 10^{-9}$ g, $h \sim 10^{-6}$ g, $a_n = 1$ μ in.)

Harmonic Number	$\Delta h = 0.01$ h (milliarc sec/yr)	$\Delta h = 0$
2	77.0	0.03
3	20.0	20.0
4	19.0	0.004
5	18.0	18.0
6	50.0	0.01
7	30.0	30.0
8	16.0	0.006
9	9.7	9.7
10	56.0	0.01
11	11.0	11.0
12	15.0	0.003
13	3.1	3.1

Finally, the factor ζ was set equal to zero for the higher harmonics, and this greatly reduced the torques for the even harmonics, as shown in Table 9. This means that the factor ζ is generally applicable and that the expression for fourth harmonic in Table 1 is probably wrong. We have not used it for computational purposes, and we include it in Table 1 to illustrate the complexity of the calculations involving higher harmonics.

To summarize, these results indicate that for the rotors considered, a preload $h \sim 10^{-6}$ g (determined primarily by roll rate), and the orientation planned for the final experiment ($\theta_0 = 45^\circ$, $\phi_0 = 0$), the drifts are of order several hundred milliarc sec/yr, two orders of magnitude larger than the experiment goal of 1 milliarc sec/yr. To reach the design goal of the experiment one must do one or a combination of three things: (1) reduce the preload, (2) align the rotor with the electrode axis (see Section VI), or (3) rely on roll averaging of torque.

While item 2 is a valid solution, it is probably too difficult to implement given the increased difficulty of reading out the gyro due to the presence of electrodes in the readout loop. Item 3 is also probably a valid solution. This is discussed in Section X.

We notice that for the second harmonic term in Table 1 and $\alpha_0 = \gamma_0 = 1/\sqrt{2}$ we have

$$\Omega = \frac{T}{I\omega} \sim \frac{1}{2\pi \sin^2 \theta_1} \frac{(2.7) (a_2)}{(2/5) r_0} \frac{\zeta h}{V} \alpha_0 \gamma_0 \sim 150 \text{ milliarc sec/yr}$$

for $a_2 = 2 \mu\text{in.}$ (due to centrifugal distortion; see Reference 4), $h = 10^{-6}$ g, $\zeta = 0.01$, $\omega = 200$ cps. So just the second harmonic gives torques of the magnitude shown in Tables 5 through 10.

The current state of the art in electrostatic gyros is of order 3×10^6 milliarc sec/yr in a 1-g environment. Scaling up the results of this section by 10^6 , we obtain drift rates of 10^8 milliarc sec/yr in a 1-g environment. Thus, the state-of-the-art rotors considered here will not have the 1-g performance of existing electrostatic gyros. This is because the current electrostatic gyros produced by Honeywell rely on gimbaling, ball balancing, centrifugal distortion compensation, and possibly computer modeling to reduce torques.

VII. TORQUE ON A GIMBALED GYRO INCLUDING ALL THE HARMONICS

We can evaluate equation (6) without resorting to a Fourier expansion for the case $\gamma_0 = 1$, $\alpha_0 = \beta_0 = 0$. In this case we have $\sin \theta = \sin \theta'$; so, neglecting the $\Delta d/d_0$ term, we obtain

$$\vec{T} = \frac{\epsilon_0 r_0^2}{2 d_0^2} \sum_i v_i^2 \int \int_{S_i} [\beta \hat{F}_x - \alpha \hat{F}_y] \frac{dr(\theta)}{d\theta} d\theta d\phi .$$

For the z+ electrode we get

$$\begin{aligned} \vec{T}_{z+} &= \frac{\epsilon_0 r_0^2}{2 d_0^2} v_{z+}^2 \left[\hat{F}_x \int_0^1 d\theta \int_0^{2\pi} d\phi \sin \theta \sin \phi \frac{dr(\theta)}{d\theta} \right. \\ &\quad \left. - \hat{F}_y \int_0^1 d\theta \int_0^{2\pi} d\phi \sin \theta \cos \phi \frac{dr(\theta)}{d\theta} \right] = 0 . \end{aligned}$$

Similarly, for the z- electrode, making the substitution $\alpha \rightarrow -\alpha$, $\gamma \rightarrow -\gamma$, we have

$$\vec{T}_{z-} = 0 .$$

For the x+ electrode we have $\alpha \rightarrow \gamma$, $\gamma \rightarrow -\alpha$; so

$$\begin{aligned} \vec{T}_{x+} &= \frac{\epsilon_0 r_0^2}{2 d_0^2} v_{x+}^2 \left[\hat{F}_x \int_0^{2\pi} d\phi \int_0^1 \sin \theta d\theta \left(\frac{\sin \theta \sin \phi dr(\theta')/d\theta'}{\sqrt{\cos^2 \theta + \sin^2 \theta \sin^2 \phi}} \right) \right. \\ &\quad \left. - \hat{F}_y \int_0^{2\pi} d\phi \int_0^1 \sin \theta d\theta \left(\frac{\cos \theta dr(\theta')/d\theta'}{\sqrt{\cos^2 \theta + \sin^2 \theta \sin^2 \phi}} \right) \right] . \end{aligned}$$

where

$$\theta' = \sin^{-1} \sqrt{\cos^2 \theta + \sin^2 \theta \sin^2 \phi} .$$

This follows since the Jacobian of the transformation is $\sin \tilde{\theta} / \sin \theta$ [1] and

$$\sin \theta = \sqrt{\alpha^2 + \beta^2} .$$

Therefore, making these substitutions gives us the radical in the denominator. Similarly, $\hat{T}_{x-} = -\hat{T}_{x+}$ so

$$\hat{T}_x = M_x [\hat{F}_x I_1 - \hat{F}_y I_2] .$$

where

$$I_1 = \int_0^{2\pi} d\phi \int_0^1 \sin \theta d\theta \left(\frac{\sin \theta \sin \phi dr(\theta')/d\theta'}{\sqrt{\cos^2 \theta + \sin^2 \theta \sin^2 \phi}} \right)$$

$$I_2 = \int_0^{2\pi} d\phi \int_0^1 \sin \theta d\theta \left(\frac{\cos \theta dr(\theta')/d\theta'}{\sqrt{\cos^2 \theta + \sin^2 \theta \sin^2 \phi}} \right) .$$

For the y+ electrode

$$\alpha \rightarrow -\beta , \quad \beta \rightarrow \gamma , \quad \gamma \rightarrow -\alpha$$

and

$$\begin{aligned} \hat{T}_{y+} = & \frac{\epsilon_0 r_0^2}{2 d_0^2} V_{y+}^2 \left[\hat{F}_x \int_0^{2\pi} d\phi \int_0^{\theta_1} \sin \theta d\theta \left(\frac{\cos \theta dr(\theta')/d\theta'}{\sqrt{\cos^2 \theta + \sin^2 \theta \sin^2 \phi}} \right) \right. \\ & \left. + \hat{F}_y \int_0^{2\pi} d\phi \int_0^{\theta_1} \sin \theta d\theta \left(\frac{\sin \theta \sin \phi dr(\theta')/d\theta'}{\sqrt{\cos^2 \theta + \sin^2 \theta \sin^2 \phi}} \right) \right]. \end{aligned}$$

For the y- electrode $\alpha \rightarrow \beta$ and $\beta \rightarrow -\gamma$; so clearly

$$\hat{T}_{y-} = -\hat{T}_{y+}$$

and

$$\hat{T}_y = M_y [\hat{F}_x I_2 + \hat{F}_y I_1]$$

The I_1 integral can easily be shown to be zero by the following argument.
The ϕ part of the integral can be written as

$$\begin{aligned} \int_0^{2\pi} f(\sin^2 \phi) \sin \phi d\phi &= \int_0^{\pi} f(\sin^2 \phi) \sin \phi d\phi \\ &+ \int_{\pi}^{2\pi} f(\sin^2 \phi) \sin \phi d\phi ; \end{aligned}$$

letting $\phi = \pi + U$ in the second integral, then $\sin \phi = -\sin U$ and the latter integral becomes

$$\int_0^{\pi} f(\sin^2 U) (-\sin U) dU$$

which exactly cancels the first integral. The final form of the torque is then

$$\vec{T} = I_2 [-M_x \hat{F}_y + M_y \hat{F}_x] \quad .$$

From Reference 1, page 137, this can be written

$$\vec{T} = \frac{I_2}{\pi \sin^2 \theta_1} [-\hat{K} \times \vec{F}] \quad .$$

where $\hat{K} = \hat{F}_z$ is a unit vector in the direction of the spin axis and \vec{F} is the force on the rotor given by equation (7). This is of the form of a mass unbalance torque for the component of unbalance along the spin axis. It includes all the harmonics through the integral I_2 , which can be evaluated exactly for any given rotor. This will lead to a drift rate of magnitude

$$\Omega = \frac{|\vec{T}|}{I\omega} = \frac{I_2}{\pi \sin^2 \theta_1} \frac{m f}{\frac{2}{5} m r_o V} = \frac{5}{2\pi \sin^2 \theta_1} \left(\frac{I_2}{r_o} \right) \frac{f}{V} \quad .$$

Using

$$f = 10^{-9} \text{ g}$$

$$V = 2400 \text{ cm/sec} \quad \text{for } \omega = 200 \text{ cps}$$

$$r_o = 0.75 \text{ in.} \quad \theta_1 = 30^\circ$$

we find

$$\Omega = (1.77 \times 10^{-9}) (I_2)$$

for I_2 in $\mu\text{in.}$ I_2 has been evaluated numerically for the three sample rotors considered earlier, and the results are

	<u>I_2</u>
Case I	0.963×10^{-6} in.
Case II	-0.710×10^{-6} in.
Case III	-0.995×10^{-6} in.

Case I $\Omega = 10.6$ milliarc sec/yr

Case II $\Omega = 7.88$ milliarc sec/yr

Case III $\Omega = 11.0$ milliarc sec/yr.

The drifts are proportional to f and $1/\omega$. So for a perfectly aligned rotor we get drift rates of the order 10 milliarc sec/yr in a 10^{-9} g environment.

The large reduction in torques for the gimbaleed case illustrates the great advantage for this orientation. This is, in fact, the orientation used for many existing electrostatic gyros and is responsible for their current excellent drift performance. These gyros use a rotor with a preferred spin axis so the axial mass unbalance torque can be minimized by balancing the ball. In fact, all the even harmonics vanish for this orientation [1]. As soon as the rotor spin axis is misaligned with the electrode axis, one picks up all the even harmonics, and these involve the relatively large preloads h . This accounts for the difference in the drifts calculated in this section and those calculated in Section VI. We can reduce the average f by drag-free control to the 10^{-10} g level, but h cannot be so reduced because of the roll of the spacecraft ($h \sim 10^{-6}$ g for 15 min roll period and 10 cm radius).

VIII. SECONDARY TORQUES

The secondary torques are by definition the torques that arise from the $\Delta d/d_0$ term in equation (6). There are four sources of secondary torques [1]:

a) Rotor asphericity:

$$\Delta d = - \Delta r(\theta') \quad .$$

where

$$\Delta r = r - r_0 \quad .$$

θ' is given by

$$\theta' = \cos^{-1} (\alpha\alpha_0 + \beta\beta_0 + \gamma\gamma_0) \quad .$$

so it is a complicated function of the direction cosines α, β, γ and $\alpha_0, \beta_0, \gamma_0$.

b) Rotor miscentering:

$$\Delta d = - \alpha x_c - \beta y_c - \gamma z_c \quad .$$

where

$$\vec{r}_c = (x_c, y_c, z_c)$$

indicates the vector from the center of the housing to the center of mass of the rotor.

c) Electrode assembly errors:

$$\Delta d = \epsilon \left\{ \frac{\Delta l}{\sqrt{6}} (\alpha + \beta + 2\gamma) + \frac{\Delta t}{\sqrt{2}} (\alpha - \beta) \right\} \quad .$$

where Δ_z is the translation of the upper hemisphere parallel to the projection of \hat{F}_z on the separation plane and Δ_\perp is the translation perpendicular to this direction, $c = +1$ for the upper half and $c = -1$ for the lower half.

d) Electrode asphericity:

$$\Delta d = R(\alpha, \beta, \gamma) \quad ,$$

where R specifies the deviations from perfect sphericity of the electrodes. This requires a model for R . Honeywell [1] has computed the torques for the (a) and (b) cases up to the sixth harmonic and in case (c) for the second and third harmonics for hexahedral electrodes. Essentially no work has been done on case (d). Extracting numerical values from these formulas is difficult and, as we have seen previously, using only the lowest harmonics is misleading.

The secondary torques could be computed exactly using the method described in Section V. One defines the three integrals

$$I_1'(\alpha_0, \beta_0, \gamma_0) = \int_0^{2\pi} d\phi \int_0^1 \sin \theta d\theta \left[\frac{\Delta d}{d_0} \alpha \frac{dr(\theta')/d\theta'}{\sin \theta'} \right]$$

$$I_2'(\alpha_0, \beta_0, \gamma_0) = \int_0^{2\pi} d\phi \int_0^1 \sin \theta d\theta \left[\frac{\Delta d}{d_0} \beta \frac{dr(\theta')/d\theta'}{\sin \theta'} \right]$$

$$I_3'(\alpha_0, \beta_0, \gamma_0) = \int_0^{2\pi} d\phi \int_0^1 \sin \theta d\theta \left[\frac{\Delta d}{d_0} \gamma \frac{dr(\theta')/d\theta'}{\sin \theta'} \right]$$

where Δd is a function of α, β, γ and $\alpha_0, \beta_0, \gamma_0$. For the four previously mentioned cases, a complete expression for the torques could then be generated by suitable permutation of the direction cosines and the I 's. Each case would have 36 terms. Note, however, that, except for case (a), upon carrying out the permutations listed in Section V, the I 's would not transform into themselves: thus, one would not have just three basic integrals. For cases (b) and (c), one would have six basic integrals (Δd proportional to either α, β , or γ); and for case (d), one would have twelve basic integrals. This is a formidable computational task that has not been carried out as yet.

One important observation about the secondary torques is that none of them averages due to spacecraft roll. This is because they contain α , β , and γ , and this destroys the averaging discussed in Section X even for the case of the rotor spin aligned perfectly with the spacecraft roll axis.

In lieu of a complete calculation of secondary torques, we can make the following observation. All the secondary torques are of order $\Delta d/d_0$ times the primary torques. So if we take the general level of primary torque drift to be of order 100 milliarc sec/yr, which would only require a slight rotor improvement, we see that $\Delta d/d_0$ need only be 1/100 to reduce the secondary torques to the milliarc sec/yr level. Since $d_0 = 1500 \mu\text{in.}$, this requires a $\Delta d \sim 10 \mu\text{in.}$ Therefore, this is the specification we will require on Δd . It is clearly satisfied for case (a). For case (b), a centering accuracy of $10 \mu\text{in.}$ is attainable, but it must be remembered that this is an absolute centering accuracy and not the stability of the centering point. The $10 \mu\text{in.}$ specification also applies to the housing centering errors and the electrode sphericity. A more definitive statement than this would require an enormous amount of numerical work. However, notice that these conclusions agree with the miscentering terms in Table 1, which are down by a factor t/d_0 from the primary torques for the lower harmonics. Also, the calculation in Reference 1 of electrode assembly errors bears out that they are down by a factor Δ/d_0 for the lower harmonics.

There is, however, a qualification to this statement because of the fact that the secondary torques, while down by a factor $\Delta d/d_0$, may not contain the reductions due to symmetry that occur in the primary torques. This is illustrated by the miscentered third harmonic term in Table 2, which contains no ζ term and is of order 15 milliarc sec/yr for $a_3 = 1 \mu\text{in.}$, $h = 10^{-6} \text{ g}$, $t/d_0 \sim 10^{-2}$; and $\omega = 200 \text{ cps}$. The higher harmonics will add to this, and the total magnitude of the drift requires the numerical integration described previously. (The miscentered second harmonic gives an insignificant drift for these same parameters and $a_2 = 2 \mu\text{in.}$ and $f \sim 10^{-9} \text{ g}$.) However, if the miscentering vector remains fixed with respect to the electrodes as the spacecraft rolls, then these miscentering torques will average to zero because they will cause no change in electrode voltages as the spacecraft rolls. These considerations indicate that a complete numerical integration for secondary torques is probably necessary.

IX, ORBITAL AVERAGING OF GRAVITY GRADIENT FORCES

The purpose of this section is to compute the average gravity gradient acceleration as a function of distance from the center of mass of the satellite. The effect of roll averaging will then be computed.

The gravity gradient acceleration \vec{f} is given by the equation

$$\vec{f} = \underline{V} \vec{\rho} \quad ,$$

where \underline{V} is a matrix of the form

$$(V)_{ij} = \frac{\partial^2 V}{\partial x^i \partial x^j}$$

and V is the gravitational potential. $\vec{\rho}$ is the vector position of the point at which the acceleration is computed with respect to the center of mass. Taking $V = GM/r$, one easily finds that for a rectangular coordinate system

$$\underline{V} = \frac{GM}{r^5} \begin{pmatrix} 3x^2 - r^2 & 3xy & 3xz \\ 3xy & 3y^2 - r^2 & 3yz \\ 3xz & 3yz & 3z^2 - r^2 \end{pmatrix} \quad .$$

We now consider a circular orbit in the y - z plane with the roll axis in the z -direction. This implies the guide star is in the orbit plane, a situation that can be realized with a suitable choice of orbit. Then for a particular point in the spacecraft specified by $\vec{\rho}$ one has

$$\rho_z = \text{const.}$$

$$\rho_y = \rho_0 \cos \omega t$$

$$\rho_x = \rho_0 \sin \omega t$$

where ω is the roll angular frequency. The orbital position is given by

$$y = R \cos \Omega t$$

$$z = R \sin \Omega t$$

$$x = 0$$

where Ω is the orbital angular frequency and R the orbital radius. Substituting this into the equation for \underline{V} and $\underline{\dot{f}}$, one obtains

$$\begin{bmatrix} f_x \\ f_y \\ f_z \end{bmatrix} = \frac{GM}{R^5} \begin{bmatrix} -R^2 \rho_0 \sin \omega t \\ R^2(3 \cos^2 \Omega t - 1) (\rho_0 \cos \omega t) + (3 R^2 \cos \Omega t \sin \Omega t) \rho_z \\ (3 R^2 \cos \Omega t \sin \Omega t) (\rho_0 \cos \omega t) + R^2(3 \sin^2 \Omega t - 1) \rho_z \end{bmatrix}$$

We can now compute the average values of these quantities, noting that

$$\langle \sin \omega t \rangle = \frac{1 - \cos \omega T}{\omega T}$$

where T is the averaging time. Similarly,

$$\begin{aligned} \langle \cos^2 \Omega t \cos \omega t \rangle &= \frac{\sin \omega T}{2 \omega T} + \frac{\sin (2\Omega - \omega) T}{4 (2\Omega - \omega) T} \\ &\quad + \frac{\sin (2\Omega + \omega) T}{4 (2\Omega + \omega) T} \end{aligned}$$

$$\begin{aligned} \langle \sin \Omega t \cos \Omega t \cos \omega t \rangle &= \frac{1 - \cos (2\Omega - \omega) T}{4 (2\Omega - \omega) T} \\ &\quad + \frac{1 - \cos (2\Omega + \omega) T}{4 (2\Omega + \omega) T} \end{aligned}$$

$$\langle \cos \Omega t \sin \Omega t \rangle = \frac{\sin^2 \Omega T}{2\Omega T}$$

$$\langle \cos \omega t \rangle = \frac{\sin \omega T}{\omega T}$$

$$\langle \sin^2 \Omega t \rangle = \frac{1}{2} - \frac{1}{4} \frac{\sin^2 \Omega T}{\Omega T}$$

We see that all components of $\langle \vec{f} \rangle$ are of order $1/\Omega T = 2\pi/\#$ of orbits or $1/\omega T = 2\pi/\#$ revolutions and thus average to zero with the very important exception of the second term in $\langle f_z \rangle$. Ignoring the term proportional to $1/\Omega T$, we have

$$\langle f_z \rangle \sim \frac{GM}{2R^3} \rho_z$$

For $\rho_z \sim 10$ cm this term is of order 10^{-8} g. We see from Section VIII that this will make a large contribution to the torque; thus, every effort should be made to minimize it.

Notice that there are $\langle f_1^2 \rangle$ terms in the expression for torque, and none of these averages to zero. However, these occur in the combination $\langle f_1^2 \rangle / h_1$. For gravity gradient forces of order 10^{-8} g and $h_1 \sim 10^{-6}$ g, these terms are of order 10^{-10} g, the same order of magnitude as the $\langle f_1 \rangle$ terms.

To summarize, we have shown that all gravity gradient accelerations average to zero under the combined effects of orbital and roll averaging with the exception of the component along the roll axis, and this can be minimized by placing all the gyros in the plane of the drag-free proof mass perpendicular to the roll axis.

For an elliptical orbit, one can write

$$\begin{bmatrix} \langle f_x \rangle \\ \langle f_y \rangle \\ \langle f_z \rangle \end{bmatrix} = GM \begin{bmatrix} -\rho_0 \langle \frac{1}{r^3} \sin \omega t \rangle \\ \rho_0 \langle \frac{3y^2 - r^2}{r^5} \cos \omega t \rangle + \langle \frac{yz}{r^5} \rangle \rho_z \\ \rho_0 \langle \frac{yz}{r^5} \cos \omega t \rangle + \langle \frac{3z^2 - r^2}{r^5} \rangle \rho_z \end{bmatrix}$$

where the average is now over an elliptical orbit. One can express y and z and thus r as a power series in the eccentricity e :

$$\frac{y}{a} = \cos \Omega t + \frac{1}{2} e (\cos 2 \Omega t - 3) + \frac{e^2}{8} (3 \cos 3 \Omega t - 3 \cos \Omega t) + \dots$$

$$\frac{z}{a} = \sin \Omega t + \frac{1}{2} e \sin 2 \Omega t + \frac{e^2}{24} (9 \sin 3 \Omega t - 15 \sin \Omega t) + \dots$$

$$r = \sqrt{y^2 + z^2} \quad a = \text{semi-major axis}$$

One can convince oneself then that

$$\left\langle \frac{1}{r^3} \sin \omega t \right\rangle \rightarrow 0$$

$$\left\langle \frac{3y^2 - r^2}{r} \cos \omega t \right\rangle \rightarrow 0$$

$$\left\langle \frac{yz}{r^5} \cos \omega t \right\rangle \rightarrow 0,$$

just as in the circular orbit case. This is because one will have terms of the form

$$\left\langle \cos^m (k \Omega t) \sin^n (l \Omega t) \cos \omega t \right\rangle,$$

where $m, n, k,$ and l are integers and these terms average to zero. So, after averaging, we obtain

$$\begin{bmatrix} \langle f_x \rangle \\ \langle f_y \rangle \\ \langle f_z \rangle \end{bmatrix} = GM \begin{bmatrix} 0 \\ \langle \frac{yz}{r^5} \rangle \rho_z \\ \langle \frac{3z^2 - r^2}{r^5} \rangle \rho_z \end{bmatrix}.$$

But $\langle \frac{yz}{r^5} \rangle$ is of order e^2/a^3 for an elliptical orbit; so $\langle f_y \rangle$ is of order $e^2 GM \rho_z / a^3$, which is small for a nearly circular orbit. Also.

$\langle \frac{3z^2 - r^2}{r^5} \rangle$ is different for a noncircular orbit. The corrections are of order e for small e . So by minimizing ρ_z we essentially eliminate the the average force in a noncircular orbit also.

While the z component of gravity gradient acceleration does not average to zero, it will not cause substantial torque on the gyro aligned with the z -axis. This can be seen by the following argument. The voltages needed to cancel the z -component of acceleration are such that for each point on the rotor the voltage is the same as for a point opposite on a line drawn through the spin axis. The torque due to the original point thus precisely cancels the torque due to the opposite point. This can be seen explicitly for the third and fifth harmonics in Table 1 which vanish for $\alpha_0 = \gamma_0 = 1/\sqrt{2}$, $\beta_0 = 0$, $M_x = M_z$, $M_y = 0$, the case appropriate for the acceleration and spin aligned with the z -axis. The even harmonics will still be there, but these are primarily due to asymmetries in the preload that would be there in any case. The non-zero $\langle f_y \rangle$ for an elliptical orbit will cause a torque on the gyro aligned with the z -axis. This acceleration is of order

$$\frac{GM}{R^3} e^2 \rho_z$$

and can be reduced to the 10^{-10} g level for $e \sim .1$. Thus, the non-zero average value of the z -component of gravity gradient acceleration will not significantly affect the gyro aligned with the z -axis from which the relativity information is extracted.

X. AVERAGING OF TORQUES DUE TO SPACECRAFT ROLL

In the final version of the gyro experiment, the spacecraft will be rolled about an axis through the guide star. This is necessary to achieve the required readout accuracy, but it is also effective in reducing the primary electrical torques on the gyro. In this section, we evaluate the effect of averaging on the torques analytically.

Consider first the case in which the gyro spin axis is perfectly aligned with the roll axis. We know that the torque is perpendicular to the roll axis. Then, if everything else is constant, the tip of the torque vector will describe a circle, and the average of the torque over one revolution will be precisely zero.

To prove this analytically we note that equation (6) is also valid in a coordinate system with the roll axis as the z-axis. Now consider an element of electrode surface described by the direction cosines α , β , γ . As the spacecraft rolls, these will vary in such a way that

$$\alpha = \sin \theta'' \cos \omega t$$

$$\beta = \sin \theta'' \sin \omega t$$

$$\gamma = \cos \theta''$$

where θ'' remains constant. The rotor spin axis is at the point midway between two adjacent electrodes; in the present coordinates this means

$$\alpha_0 = \beta_0 = 0.$$

Hence $\theta' = \theta'' = \text{constant}$. Thus, if the V_i 's remain constant in equation (6) then averaging over one roll we have

$$\langle \alpha \rangle = 0 \quad \langle \beta \rangle = 0$$

Since this holds for each element of electrode area, we have (neglecting $\Delta d/d_0$ terms)

$$\langle \vec{T} \rangle = 0$$

for one complete revolution. At any given point the torque is reduced by a factor $\sim 1/n$ of its static value, so that for 10^4 revolutions (~ 1 yr for 15 min roll period) the torques are reduced by four orders of magnitude. This holds only if the V_i 's remain constant, which is the case for the centrifugal accelerations due to the roll. It is not true for other accelerations, but these are taken care of by the drag-free proof mass and the gravity gradient acceleration averaging as described in Section IX. The averaging also does not hold for the secondary torques ($\Delta d/d_0$ terms), since these terms may contain, α , β and γ and thus destroy the averaging. An important example of this is miscentering torques (see Section VIII).

If the rotor spin axis is not precisely aligned with the roll axis, then $\alpha_0 \neq 0$, $\beta_0 \neq 0$ and we get terms which do not average to zero, since $\gamma\alpha_0$ and $\gamma\beta_0$ terms are present, and also θ now varies as the spacecraft rolls. These terms are very difficult to compute, but we see they are of order α_0 or β_0 times the primary torques. For example, for a 10 arc sec misalignment of the rotor spin axis, α_0 and β_0 are of order 5×10^{-5} , so the nonaveraged part of the torques are reduced by this factor relative to the static primary torques.

Thus, we conclude that roll averaging is extremely effective in reducing torques provided the spin axis can be kept aligned closely to the roll axis. This statement applies only to the primary torques and requires that the preloads remain nearly constant during one roll period.

We can thus see that the effect of rolling the spacecraft is to eliminate the first h_i term in equation (9); therefore, we have run our program with this term set equal to zero. The results are shown in Table 10. They indicate that the drift rates can be reduced to the milli-arc sec/yr level for $f \sim 10^{-9}$ g for the rotors considered here. We also note that the higher harmonics are not very significant. This was also the case for the torques before averaging when the relatively large second harmonic due to centrifugal distortion dominated the torque expression. This term is of order 2 μ in. for $\omega = 200$ cps and was included in the previous calculations of Tables 5 through 8. We conclude that milliarc sec/yr drifts are feasible for $f \sim 10^{-9}$ g after averaging due to roll is accounted for. Roll averaging of secondary torques could be accounted for also by setting $h_i = 0$ in equation (9) and performing the integrations described in Section VIII.

TABLE X. DRIFT RATES AFTER AVERAGING

Average f (g's)	Case I	Case II (milliarc sec/yr)	Case III
10^{-8}	11.0	34.0	86.0
10^{-9}	0.89	1.2	4.4
10^{-10}	0.089	0.12	0.44

XI. SPIN AVERAGING

Honeywell [1] has given a proof that if the rotor is spinning sufficiently fast, then one can assume that the rotor is axially symmetric with a shape given by

$$\bar{r}(\theta) = \frac{1}{2\pi} \int_0^{2\pi} r(\theta, \phi) d\phi,$$

where $r(\theta, \phi)$ is the actual ball shape in terms of θ and ϕ . This is valid provided

$$\frac{d\bar{r}(\theta)}{d\theta} \gg \frac{1}{\pi d_0} \int_0^{2\pi} \Lambda(\theta', \zeta) \frac{\partial \Delta(\theta', \zeta)}{\partial \theta'} d\zeta,$$

where

$$\Delta(\theta, \phi) = r(\theta, \phi) - \bar{r}(\theta).$$

Reference 1 refers to this as a "locally smooth" condition. To obtain the appropriate input for the torque calculation, one must compute $\bar{r}(\theta)$. This requires a complete map of the ball in θ and ϕ , which is not currently available. For the purposes of this report, we have used $r(\theta, \phi_0)$ for $0 < \theta < \pi$ and some ϕ_0 instead of $\bar{r}(\theta)$. Undoubtedly some averaging occurs in the integral of $\bar{r}(\theta)$ that will improve the effective smoothness of the ball, but it is difficult to estimate how much until a complete map of the ball is available. A numerical integration to determine $\bar{r}(\theta)$ will then be required.

XII. CONCLUSION

The main conclusion of this report is that Newtonian electrical torques permit drift rates of order several hundred milliarc sec/yr with preloads of $10^{-6}g$ and existing rotors. The preload setting is determined by safety considerations, and the roll rate, and correspondingly better drift rates are possible with lower preload settings. Roll averaging will reduce the primary torques to well below the 1 milliarc sec/yr level. The secondary torques are at the 1 milliarc sec/yr level for existing rotors, assuming a fractional uniformity of rotor electrode gap of 1/100. The gravity gradient forces average out when combined with the spacecraft roll except for the component along the roll axis. This component, however, does not produce significant torque on the gyro aligned with the roll axis from which the relativity information is extracted. The effects due to spin averaging of the rotor asphericity may lower the drift rates calculated here, but this calculation awaits a complete map of the rotor. The overall conclusion is that, from the point of view of electrical torque calculations, an accuracy of 1 milliarc sec/yr drift is a feasible goal for the gyro experiment.

REFERENCES

1. Matchett, G.A.: Honeywell Report 20831FR, Vol. II, NASA Contract NAS-12-542, November 1968.
2. Everitt, C.W.F.: Conference on Experimental Tests of Gravitational Theories, November 1970, JPL TM33499.
3. Spencer, Tom: Ball Brothers Contract Report F7303.
4. Eby, P.: NASA TMX-64964, November 1975.

APPENDIX

PRECEDING PAGE BLANK NOT FILMED

00333	1100	TOT= SORT (TR0TR0TV0V0720T7)	001360
00334	1150	WRITE (6,220) TOT	001375
00337	1100	667 CONTINUE	001006
00340	1170	648 CONTINUE	001004
00341	1180	0777 J=1,97	001004
00348	1150	FMCAJ35C05125,03M1J11	001908
00345	1200	77 CONTINUE	001015
00347	1210	CALL NEWCO	001015
00350	1220	WRITE (6,220) D SORT	001017
00353	1230	STOP	001025
00354	1240	END	001031

END OF COMPILATION: 3 DIAGNOSTICS.

JPOP.15 MEMCO
MSA_K1-07/22/79-17:22:39.1.01

SUBROUTINE MEMCO ENTRY POINT 000066

STORAGE USED: CODE(1) 000077; DATA(0) 000371; COMMON(2) 000000

COMMON BLOCKS:
0003 NAME13 000156
0004 NAME16 000007

EXTERNAL REFERENCES (BLOCK, NAME)

0005 MERR11

STORAGE ASSIGNMENT (BLOCK, TYPE, RELATIVE LOCATION, NAME)

0001	000005	1106	COCD R 000003 AF1	0000 R 000004 AF2	0000 R 000005 AF3	0000 R 000006 AF4
0002	000007	AF5	0000 000001 B262	0003 R 000142 DEL	0003 R 000000 DSDTT	0000 R 000002 FACT
0003	R 000001	FMC	0000 000020 IMJPS	0000 I 000000 JJ	0000 I 000001 M	0000 000000 TL

00101	10	SUBROUTINE MEMCO	000000
00103	20	COMMON/NAME13/DSDTT,FMC(17),DFL(17)	000000
00104	30	COMMON/NAME16/TL,B262	000000
00105	40	JJ=1	000000
00106	50	DSDTT=0	000001
00107	60	DO 1 N=1,12	000005
00112	70	FACT=0,DFL(1)/16175.	000005
00113	80	JJ=JJ+8	000010
00114	90	AF1=FMC(JJ-8) * FMC(JJ)	000018
00115	100	AF2=FMC(JJ-7) * FMC(JJ-1)	000017
00116	110	AF3=FMC(JJ-6) * FMC(JJ-2)	000022
00117	120	AF4=FMC(JJ-5) * FMC(JJ-3)	000025
00120	130	AF5=FMC(JJ-4)	000030
00121	140	DSDTT=DSDTT + FACT(1009,0AF1+5000,0AF2+928,0AF3+10096,0AF4	000032
00121	150	1-9590, 0AF5)	000032
00122	160	1 CONTINUE	000067
00124	170	RETURN	000007
00125	180	END	000076

END OF COMPILATION: NO DIAGNOSTICS.

FORM 15 P1
 USA 11-01222279-17122139 1.0J

FUNCTION P1 ENTRY POINT 000221

STORED USER CODE 111 000422; DATA(01 000209) BLANK COMMON(12) 000000

COMMON BLOCKS:

0001 NAME1 000101
 0004 NAME10 000024
 0005 NAME11 000172
 0006 NAME11 000602
 0007 NAME2 000155
 0010 NAME14 000014

EXTERNAL REFERENCES (BLOCK, NAME):

0011 MEMCO
 0012 COS
 0013 S14
 0014 ACOS
 0015 RELR34

STORAGE ASSIGNMENT (BLOCK, TYPE, RELATIVE LOCATION, NAME):

0001 000002 1136 0001 000011 1206 0001 000022 1236 0001 000113 1336 0001 000144 1506
 0001 000017A 1556 0000 P 000152 RJ 0010 B 000000 DAL 0007 P 000151 DEL
 0005 W 000000 05011 0000 B 000107 E 0005 B 000001 FMC 0000 B 000000 F1
 0000 I 000195 J 0000 000157 14JPS 0000 J 000151 J 0000 I 000193 JK
 0000 Y 000192 M 0000 I 000154 MM 0000 I 000106 L 0000 B 000000 P
 0004 000000 RJ 0000 P 000150 S 0005 B 022301 S1 0001 B 000000 TP
 0005 000156 VSS

0001 10 FUNCTION F1(A,B,C)
 0003 20 COMMON/NAME1/Y(197)
 0010 30 COMMON/NAME10/P(120)
 0015 40 COMMON/NAME11/D(50),FMC(197),DEL(12),VSS(12)
 0020 50 COMMON/NAME11/R(197,977),S(197,97)
 0017 60 COMMON/NAME2/Y(197),D(11)
 0011 70 COMMON/NAME13/DAL(12)
 0012 80 DIMENSION GNC(97)
 0015 100 ON 070 H=1,12
 0017 110 DEL(1)=DAL(1)
 0022 120 DO 90 JK=1,97
 0025 130 I=JK
 0027 140 L=JK
 0014 150 L=RSJIMTMIJ10COSITMILJ10OSITMILJ10OSITMILJ10COSITMILJ10
 0014 160 E=ACOS(E)

00131	170	S=0	00103
00132	180	DO 70 AFI .20	00113
00133	190	AJ=F	00113
00134	200	S =S -JOP(JLO SIMLAPOE)	00116
00137	210	70 CONTINUE	00136
00138	220	SILLLES	00136
00142	230	80 FNC(JM)=SI(JM,JL)OSTMTH(JM)OCOS(ITM(JL)OSTM(ITM(JM))SINIE)	00140
00144	240	CALL NENCO	00153
00146	250	90 GNC(JL)=DSOTI	00155
00147	260	DO 97 LH=1-12	00160
00152	270	97 OFL(LM)=DIL(LM)	00160
00153	280	DO 98 RM=1-97	00171
00157	290	98 FNC(RM)=GNC(RM)	00171
00161	300	CALL NENCO	00173
00162	310	FIDSDIT	00175
00163	320	RETURN	002177
00164	330	END	00201

END OF COMPILATION: NO DIAGNOSTICS.

3809.15 F2

MSA F3 -01/22/79-17:22:03.1.01

FUNCTION F2 ENTRY POINT 000721

STORAGE USED: CODE(1) 000242; DATA(1) 000204; CLAMP COMMON(1) 000000

COMMON BLOCKS:

C001 NAME1 000101
 C002 NAME10 000029
 C003 NAME13 000172
 C006 NAME11 000602
 C007 NAME2 000155
 C010 NAME14 000014

EXTERNAL REFERENCES (BLOCK, NAME)

C011 MEMCO
 C012 SIN
 C013 COS
 C014 ACOS
 C015 MERR33

STORAGE ASSIGNMENT (BLOCK, TYPE, RELATIVE LOCATION, NAME)

U001	000002	1136	0001	000011	1206	0001	030022	1236	0701	000113	1336	0001	000164	1506	
U002	000171	1556	0000	R	000152	AJ	0010	P	000000	DAL	0005	P	000142	DEL	
U003	R	000000	05077	0000	R	000147	E	0005	P	000001	FMC	0000	P	000001	GMC
U004	I	000145	I	0000	000157	INJPS	0000	I	000151	J	0000	I	000144	JL	
U005	I	000142	K	0000	T	000154	MM	0000	I	000146	L	0000	P	000000	P
U006	000000	R1	0000	P	000150	S	0006	R	022301	S1	0003	P	000000	TM	
U005	000156	V55													

U0101	10	FUNCTION	FZ(A,B,C)											000002
U0102	20	COMMON/NAME1	/TR(97)											000002
U0103	30	COMMON/NAME10	/P(20)											000002
U0104	40	COMMON/NAME13	/OSDT,FMC(97),DFL(17),V55(12)											000002
U0105	50	COMMON/NAME11	/R(1,97,97),S(1,97,97)											000002
U0106	60	COMMON/NAME2	/TR(97),DEL(17)											000002
U0107	70	COMMON/NAME14	/DEL(12)											000002
U0108	80	DIMENSION	GMC(97)											000002
U0109	90	DO	970	N=1,12										000002
U0110	100	DEL	(K)=DALINI											000002
U0111	110	DO	90	JL=1,97										000002
U0112	120	DO	90	JM=1,97										000002
U0113	130	J=JM												000002
U0114	140	LEA												000002
U0115	150	E=ASIN(TM(1))	0COS(TM(1))	0SIN(TM(1))	0SIN(TM(1))	0COS(TM(1))	000002							
U0116	160	E=ACOS(E)												000002

00131	170	S=0	000103
07132	180	00 70 J=1,20	000113
00133	190	AJ=J	000113
00134	200	S=FS -JOP(J)SINIAJZE1	000116
00137	210	70 CONTINUE	000136
00138	220	SILLALJ=5	000136
00139	230	80 FNC(J)=S11JM.JL10SINITH(JM1)0SINITH(JM1)75INIE1	000140
00140	240	CALLNENCO	000153
07141	250	90 GNC(JL)=DSOIT	000155
00142	260	DO7 LK=1,12	070160
00143	270	DEL(LR)=OIL(LR)	000160
00144	280	DO 98 MR=1,97	000171
00145	290	98 FNC(M)=GNC(M)	000171
00146	300	CALL NENCO	000173
00147	310	F2=DSOIT	000175
00148	320	RETURN	000177
00149	330	END	000241

END OF COMPILATION NO DIAGNOSTICS

ORIGINAL PAGE IS
OF POOR QUALITY

00131	170	S=0	000064
00132	180	DO 70 J=1.20	000076
00133	190	A=J	000076
00134	200	S=5	000101
00135	210	70 CONTINUE	000121
00136	220	SLLI,LLIS	000121
00137	230	90 FNCI(J)=S1(J),J,1)COSI(7(J),J))OSI(7(J),J)))/S1(J)	000123
00138	240	CALLMEBCO	000151
00139	250	90 GNCI(J)=OSI(7	000153
00140	260	DO 7 LR=1,12	000162
00141	270	97 OFL(1)=OR(LR)	000162
00142	280	DO 99 RR=1,97	000167
00143	290	98 FNCI(M)=GNCI(M)	000167
00144	300	CALL WNCO	000171
00145	310	PS=OSI(7	000173
00146	320	RETURN	000175
00147	330	END	000235

END OF COMPILATION: NO DIAGNOSTICS.

APPROVAL

ELECTRICAL TORQUES ON THE ELECTROSTATIC GYRO IN THE GYRO RELATIVITY EXPERIMENT

By Peter Eby and Wesley Darbro

The information in this report has been reviewed for technical content. Review of any information concerning Department of Defense or nuclear energy activities or programs has been made by the MSFC Security Classification Officer. This report, in its entirety, has been determined to be unclassified.

Eugene W. Urban

EUGENE W. URBAN
Chief, Cryogenic Physics Branch

Rudolf Decher

RUDOLF DECHER
Chief, Space Physics Division

Charles A. Lundquist

CHARLES A. LUNDQUIST
Director, Space Sciences Laboratory

PRECEDING PAGE BLANK NOT FILMED